Model reduction book volume II
De Gruyter Studium

Editor in Chief

Volume

Model reduction book volume II

Edited by

Editors



Mathematics Subject Classification 2010

ISBN
e-ISBN (PDF)
ISSN

Library of Congress Cataloging-in-Publication Data
A CIP catalog record for this book has been applied for at the Library of Congress.

Bibliographic information published by the Deutsche Nationalbibliothek
The Deutsche Nationalbibliothek lists this publication in the Deutsche Nationalbibliografie; detailed bibliographic data are available on the Internet at http://dnb.dnb.de.

© 2019 , Walter de Gruyter GmbH, Berlin/Boston
Cover image:
Typesetting:
Printing and binding:
♾ Printed on acid-free paper
Printed in Germany

www.degruyter.com

…
…

Elke Deckers, Wim Desmet, Karl Meerbergen*, and Frank Naets

Case studies of model order reduction for acoustics and vibrations

Abstract: This chapter presents several case studies to illustrate specific aspects in setting up reduced order models of acoustic and vibration models in mechanical applications. Modal truncation approaches have been a proven workhorse for over half a century in civil and mechanical engineering, but, for many (recent) applications, these techniques are too limited. In mechanical engineering, model users are interested in a range of model applications: frequency- and time-domain, linear and nonlinear, single domain and multi-physics, etc. This broad range of applications makes it particularly challenging to devise appropriate ROM schemes, as a scheme for one model use might be completely inadequate for other applications. Krylov methods for example have been a go-to technique in many domains, but face particular challenges in mechanical finite element models as the system's eigenvalues lie along the imaginary axis and the high frequencies are irrelevant for a given mesh size from a physical perspective. In the current chapter we explore these particularities for different types of mechanical models and simulation purposes, in order to surface several good practices and points of attention when applying model order reduction on these models. We bring together two different viewpoints: the application of model order reduction from a purely mathematical point of view and the physical interpretation of models and expected properties of reduced order models based on physical arguments from the field of mechanics. While we touch upon a range of novel model order reduction techniques, we do not discuss parametric model order reduction as it is expected that the presented guidelines can be exploited in parametric problems without additional specific concerns.

Elke Deckers, Wim Desmet, Frank Naets, KU Leuven, Department of Mechanical Engineering, Leuven, Belgium

***Corresponding author: Karl Meerbergen,** KU Leuven, Department of Computer Science, Leuven, Belgium

DOI 10.1515/-1

1 Overview of mechanical vibration and acoustic applications and models

1.1 Introduction

The modeling of the vibrational and acoustic behaviour of physical systems is far from trivial. In a general coupled vibro-acoustic system, in which a structure and acoustic cavities mutually interact with each other, the system behaviour is typically determined by the coupled response of each of the components, often requiring an accurate representation of the interface. For acoustic simulations, the frequency range of interest typically runs up to 20kHz. In real life, however, this range cannot be covered due to the limitations of the current Computer Aided Engineering tools. Moreover, there is a significantly different response in different frequency regions. In general, three different frequency regions can be identified, also visualised in Figure 1 which are typically problem dependent:

Low frequency range In the low frequency range, the characteristic length of the problem under study is smaller than or in the same order of magnitude as the dominant physical wavelengths in the dynamic response. In this frequency range, the response of the system is determined by well-separated eigenvalues or modes and can be predicted by means of deterministic approaches. For vibro-acoustic problems, element based techniques, such as the Finite Element Method (FEM) [60] and the Boundary Element Method (BEM) [55] are most commonly applied. Element based approaches divide the problem domain or its boundary into a large number of small elements. Inside these elements, the field variables are approximated using simple, often polynomial, functions. As wavelenghts shorten with increasing frequency, the element size also needs to decrease to diminish the effect of interpolation and pollution errors [18, 31]. As a consequence, the number of Degrees Of Freedom (DOFs) increases, as does the size of the system matrices, limiting the practical use of element based approaches to lower frequency applications.

High frequency range When the characteristic length of the problem under study is much larger than the dominant physical wavelengths in the dynamic response, the considered problem is situated in the high frequency range. Typically, the modal density and modal overlap are high and the system is very sensitive to small variations in for instance material properties and geometrical details. As small variabilities are inevitable in real life applications, the response of one nominal system loses its meaning. As a result, the spatially averaged response of a number of realisations is of interest together with its variance. In this frequency range, statistical techniques are applied;

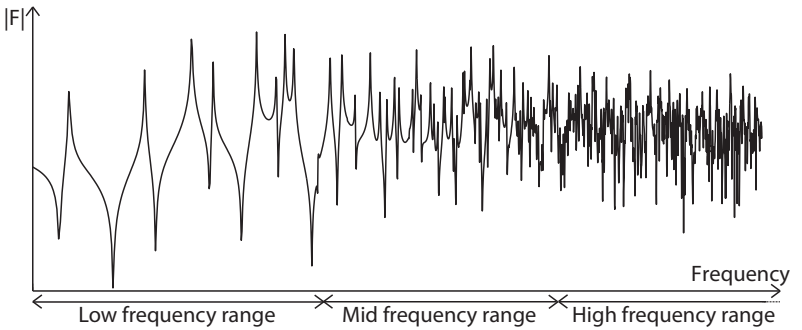


Fig. 1: Typical frequency response function of weakly damped mechanical vibrational system [54]

for instance the Statistical Energy Analysis (SEA) [29] is often used for vibro-acoustic analysis. The SEA divides the problem domain into a small number of subsystems in which a spatially averaged estimate of the energy level is obtained. SEA is computationally not demanding, but relies on a number of assumptions, such as for instance a high modal overlap and an energetic similarity of the different subsystems. Since these assumptions are only met above a certain frequency limit, the method is restricted to the high frequency range.

Mid frequency range In-between the low and the high frequency range, a frequency band exists for which it is stated that currently no mature and adequate prediction techniques are available. However, for many applications, this mid frequency gap coincides with the frequency range where the human perception and hearing is highly sensitive. Therefore, solutions are sought to bridge (part of) this gap. One approach is to increase the frequency range of the deterministic approaches by increasing the size of the resulting models. Here, amongst others, model order reduction can be an important enabler.

This chapter will focus on model order reduction techniques for vibrational and acoustic systems in the low to mid frequency range. Typically, these FE models of vibrational and acoustic systems result in a system of second order ordinary differential equations with large, but sparsely populated system matrices that allow for efficient solution algorithms. If no complex damping treatments are considered, the obtained models are linear and frequency-independent. FE models can easily be represented as linear state-space systems. The system matrices of a BE model are in general smaller (as only the boundary of the domain has to be

discretised into elements resulting in a substantially lower amount of DOFs) than their FE counterpart. However, the BE matrices are fully populated and have a rather complex frequency dependence. For this reason, it is not straightforward to convert BE equations to a time domain equivalent. This sometimes makes this approach inadequate for engineering applications.

Given the properties listed above, the maturity and the widespread industrial use of FEM, make it very accessible for practical problems. This is why only FE models are considered in this chapter.

Besides component model analysis acceleration, reduced order vibrational and acoustic models are a key enabler for many integrated simulation applications. In flexible multibody simulation, reduced order vibrational component models are exploited in order to allow for the inclusion of coupled body flexibility in a mechanical system level context, as discussed in Chapter Rixen. The analysis and design of new materials requires multi-scale simulation where model reduction has the potential to allow to bridge these different scales in a fully coupled framework [59]. Overall, these Reduced Order Model (ROM) approaches can be considered as a key enabler for current and future applications where vibro-acoustic models need to be evaluated in a broader system level performance context.

1.2 Mathematical models of vibrational, acoustic and vibro-acoustic systems

1.2.1 Vibrational problem definition

By combining constitutive equations based on Hooke's law, which expresses that the relationship between stress and strain is linear, and momentum equations, the elastic wave equation is obtained [4]:

$$\rho \frac{\partial^2 \vec{u}}{\partial t^2} = (\lambda_L + 2\mu_L) \overrightarrow{\nabla} \left(\overrightarrow{\nabla} \cdot \vec{u} \right) - \mu_L \overrightarrow{\nabla} \times \overrightarrow{\nabla} \times \vec{u} + \vec{F_b} \,, \tag{1}$$

in which $\vec{u}$ describes the solid displacement in the three spatial dimensions, $\vec{F_b}$ is the body force per unit volume acting on the solid, and λ_L and μ_L are the Lamé coefficients of the isotropic material.

For some commonly encountered geometries in vibrational problems, this elastic wave equation can be simplified. If the geometrical domain is much smaller in one direction than the other two, Kirchchoff-Love plate theory [48] can be applied, considering only bending due to transverse loads for plates subject to small deformations. It is explicitly assumed that straight cross-sections remain straight under deformation, including no shear effects. In this case, the equation

of motion is given by:

$$D\left(\frac{\partial^4 u}{\partial x^4} + 2\frac{\partial^4 u}{\partial x^2 \partial y^2} + \frac{\partial^4 u}{\partial y^4}\right) = -\rho\frac{\partial^2 u}{\partial t^2} + F_t \ , \tag{2}$$

where u is now only the (scalar) transverse displacement, x and y describe the in-plane location, F_t is the transverse load expressed as a force per unit area, ρ is the mass per unit area and D is the plate bending stiffness, being defined as:

$$D = \frac{Eh^3}{12(1-\nu^2)} \, , \tag{3}$$

where h is the plate thickness, E the plate material Young's modulus and ν is its Poisson's ratio. As the Kirchchoff-Love plate equation (2) is a fourth-order differential equation, two boundary conditions have to be applied at each location on the boundary to have a well-posed problem. Commonly applied boundary conditions are free edges, clamped edges and simply supported edges. Next to plates, often shells are applied. The difference with plates is that for shells also in-plane deformations and stresses are modeled. These types of models are often used to represent thin-walled structures, increasing computational efficiency. Thin-walled structures are often encountered in vibro-acoustic applications. Shell structures are in general quite stiff in-plane, and more flexible out-of-plane. These types of structural models are typical for mechanical and civil engineering applications and are not often encountered in other disciplines. They moreover tend to couple strongly to the acoustic domain.

1.2.2 Acoustic problem definition

The constitutive equation in acoustics is the so-called acoustic wave equation:

$$\overrightarrow{\nabla}^2 p - \frac{1}{c^2}\frac{\partial^2 p}{\partial t^2} = -\rho_0 \frac{\partial q}{\partial t} \, , \tag{4}$$

which has to be solved in order to obtain the sound pressure $p(x, y, z, t)$ in a given system, being the pressure perturbation around the ambient reference state p_0. In this equation, $\overrightarrow{\nabla}^2$ is the Laplace operator which is defined as $\overrightarrow{\nabla}^2 = \frac{\partial^2}{\partial x^2} + \frac{\partial^2}{\partial y^2} + \frac{\partial^2}{\partial z^2}$, ρ_0 is the ambient fluid density, q is the flow rate (m^3/s) of an acoustic volume source and c is the speed of sound, defined as:

$$c = \sqrt{\frac{\gamma p_0}{\rho_0}} \, , \tag{5}$$

where γ is an inherent property of the studied gas, being the ratio of the specific heat capacity for constant pressure and the specific heat capacity for constant volume.

The acoustic wave equation (4) assumes the fluid to behave as an ideal gas, assumes that pressure changes in acoustics are adiabatic and the fluid flow to be inviscid. More details can be found in e.g. [10].

Acoustics are often studied in the frequency domain. Assuming a time-harmonic $e^{\jmath\omega t}$-dependence of the dynamic quantities and excitations, the inhomogeneous Helmholtz equation is retrieved [41]:

$$\overrightarrow{\bigtriangledown}^2 p(\omega) + k^2 p(\omega) = -\jmath\rho_0\omega q(\omega)\,, \tag{6}$$

where

$$k = \frac{\omega}{c} = \frac{2\pi f}{c}\,, \tag{7}$$

is the acoustic wavenumber at frequency f. The acoustic wavelength λ, is defined in terms of the speed of sound and the frequency as

$$\lambda = \frac{c}{f}\,. \tag{8}$$

The Helmholtz equation (6) is a second order differential equation, meaning that one boundary condition has to be specified at each point of the boundary in order to obtain a well posed problem. Typically, for bounded acoustic problems, Neumann, Dirichlet and Robin boundary conditions are applied.

1.2.3 Vibro-acoustic coupling

When strong vibro-acoustic coupling is considered, it is assumed that vibrations induce acoustic waves, but that the acoustic field in turn also excites structural vibrations. This is often the case for closed cavities and thin-walled structures, as often encountered in mechanical application like car interior cavities. In a coupled vibro-acoustic system, the pressure field p in the acoustic domain and the elastic displacements $\vec{u}$ mutually affect each other on the wetted interface:

- the structural out of plane velocity $\dot{u}$ on the wetted structure is seen as an imposed velocity for the acoustic domain;
- the acoustic pressure field p on the wetted structure is considered as a distributed load on the structural domain.

1.3 Finite element modeling and discretization

1.3.1 General formulation

The modeling procedure of the FEM can be applied to any general set of (coupled) differential equations. In a first step, the problem domain is discretised into a large number of small elements which are interconnected by a network of n_{fe} nodes. Each field variable $v_i(\vec{r})$ at location $\vec{r}$ is approximated in each of the elements by a solution expansion $\hat{v}_i(\vec{r})$ in terms of n_{fe} (polynomial) shape functions N_{f_i}:

$$\begin{aligned} v_i(\vec{r}) \simeq \hat{v}_i(\vec{r}) &= \sum_{f_i=1}^{n_{\text{fe}}} N_{f_i}(\vec{r}) v_{f_i} \\ &= \mathbf{N}_i(\vec{r})\mathbf{v}_i. \end{aligned} \tag{9}$$

The nodal values v_{f_i} belonging to each of the n_{fe} nodes are gathered in the vector of the (generalized) degrees-of-freedom $\mathbf{v}_i$. The row vector $\vec{N}_i$ collects the n_{fe} shape functions N_{f_i}. These shape functions only have a non-zero value inside the element to which they belong. Moreover, each shape function has a value of 1 for only one DOF of the element and is zero at all others. The polynomial shape functions do not exactly satisfy the differential equations describing the physical problem to solve, nor the imposed boundary conditions. Typically, a weighted residual formulation is applied, and these errors are orthogonalised with respect to a set of weighting functions and minimised. In the FEM, typically a Galerkin weighted procedure is applied, expanding the weighting functions in terms of the same locally defined shape functions as for the field variables.

The FEM approach allows to generate models for the structural and acoustic problem both in the time and frequency domain with a total of n degrees-of-freedom. For the time domain simulation, the resulting (semi-discretized) model is obtained as:

$$\mathbf{M}\ddot{\mathbf{x}} + \mathbf{C}\dot{\mathbf{x}} + \mathbf{K}\mathbf{x} = \mathbf{f}, \tag{10}$$

with $\mathbf{K} \in \mathbb{R}^{n\times n}$ the stiffness matrix, $\mathbf{C} \in \mathbb{R}^{n\times n}$ the damping matrix and $\mathbf{M} \in \mathbb{R}^{n\times n}$ the mass matrix, and $\ddot{\mathbf{x}}$ and $\dot{\mathbf{x}}$ representing respectively the first and second time derivatives of the nodal time-domain degrees-of-freedom $\mathbf{x} \in \mathbb{R}^n$, with external (time-domain) loads $\mathbf{f} \in \mathbb{R}^n$.

In the frequency domain, the resulting discretized model becomes:

$$(\mathbf{K} + \jmath\omega\mathbf{C} - \omega^2\mathbf{M})\mathbf{x} = \mathbf{f} \tag{11}$$

with $\mathbf{x}$ and $\mathbf{f}$ now represented in the frequency domain. In general vibro-acoustic problems the model matrices $\mathbf{K}$, $\mathbf{C}$ and $\mathbf{M}$ can moreover be frequency dependent

as well. In the remainder of this chapter we will mainly focus on this frequency dependent problem, as many of the time-domain aspects have been covered already in Chapter Rixen. Nevertheless, several additional points are raised, specifically focusing on converting these frequency-domain models into equivalent time-domain models.

1.3.2 Properties

The discretisation strategy of the FEM and the use of simple polynomial interpolation functions has its advantages and disadvantages. In practice this approach leads to the following general characteristics:

Problem discretization and degrees of freedom – The FE approach divides the problem domain into a large number of small elements. The DOFs in an FE model are the nodal values of the field variables, and inside the elements, the dynamic field is approximated using simple polynomial shape functions. As frequencies of interest increase and wavelengths shorten, the FE mesh needs to be refined to retain a sufficient accuracy as driven by interpolation and pollution errors [18, 31]. Practically, for linear elements, a rule of thumb is to apply at least 10 element per wavelength. Calculations at higher frequencies than considered by this rule-of-thumb for a given mesh can be considered erroneous and are physically not meaningful.

Problem geometric complexity – Due to the fine discretization typically necessary to capture the wavelengths, the FEM has almost no restrictions regarding the geometrical complexity, as the elements are required to be small anyhow.

System matrix properties – In general, for undamped, viscously damped or proportionally damped structures, the system matrices of the uncoupled acoustic and structural FE model are real-valued, large, frequency independent, symmetric, and sparsely populated with a banded structure. These properties allow for an efficient storage, solution and reuse of the matrices for different frequencies [60].

Computational performance – Although the FE matrices are in general sparse and symmetric, because of the large number of FE degrees of freedom, the solution of the FE models is still computationally demanding. The CPU time required to build and solve the system is proportional to $n\Delta^2$, with n the number of DOFs for the FEM and Δ the bandwidth of the system matrix.

1.3.3 Vibro-acoustic coupling

The uncoupled acoustic and structural subproblem result in systems of equations of the format presented in equation ((10)-11), in which the primary variables for the acoustic domain are the nodal pressure vector $\mathbf{p}$ and for the structural domain the structural displacement vector $\mathbf{u}$. By accounting for the coupling conditions between both domains, the following FE system of equations is obtained in the frequency domain:

$$\left(\begin{bmatrix} \mathbf{K}_s & \mathbf{K}_c \\ 0 & \mathbf{K}_a \end{bmatrix} + \jmath\omega \begin{bmatrix} \mathbf{C}_s & 0 \\ 0 & \mathbf{C}_a \end{bmatrix} - \omega^2 \begin{bmatrix} \mathbf{M}_s & 0 \\ -\rho_0 \mathbf{K}_c^T & \mathbf{M}_a \end{bmatrix} \right) \begin{bmatrix} \mathbf{u} \\ \mathbf{p} \end{bmatrix} = \begin{bmatrix} \mathbf{f}_s \\ \mathbf{f}_a \end{bmatrix}, \tag{12}$$

where the subscript a, s and c respectively denote the uncoupled acoustic and structural system matrices and the coupling matrices, respectively. Equation (12) can be written more compactly as

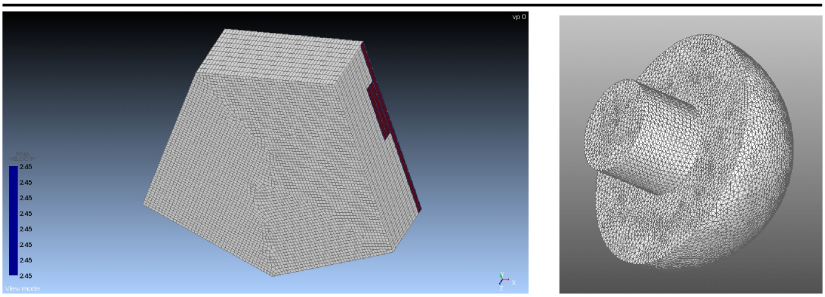
$$\left(\mathbf{K}_{up} + \jmath\omega \mathbf{C}_{up} - \omega^2 \mathbf{M}_{up} \right) \mathbf{x}_{up} = \mathbf{f}_{up}\,, \tag{13}$$

where the subscript up refers to the use of the structural displacements and acoustic pressure as primary field variables in the structural and acoustic subproblems, respectively. This system of equations has the same shape as the uncoupled structural dynamic and acoustic finite element models. The coupled system matrices are still sparse and frequency independent [12]. It is worth noting that the coupled stiffness matrix $\mathbf{K}_{up}$ and mass matrix $\mathbf{M}_{up}$ are no longer symmetric due to the presence of the coupling matrix $\mathbf{K}_c$.

2 General comments on model order reduction for vibrations

2.1 Choice of linear system solver

Before we dive into model order reduction methods, a comment on the solution of a sparse linear system is in order. The linear system of Eq. (11) is usually hard to solve by an iterative method, even for low frequencies. The condition number of the frequency dependent system matrix is usually high and the matrix is often far from definite. An additional difficulty is that classical preconditioners, such as multigrid and incomplete factorizations, are often only reliable when specific mathematical properties are satisfied, such as (positive) definiteness or the **M**-matrix property. The literature proposes techniques to overcome this difficulty by applying these preconditioner to another, modified system matrix that is more



a. [33] b. [34]

Fig. 2: Meshes for liner solver benchmarks

favourable to preconditioning. For undamped acoustics, ($\mathbf{C} = 0$), the incomplete factorization was applied to $\mathbf{K} + \alpha^2\mathbf{M}$ [30] with an optimal choice of α, which is currently known as the shifted Laplace preconditioner. For damped acoustics with nonzero $\mathbf{C}$, one could apply the preconditioner to $\mathbf{K} + \jmath\omega\mathbf{C} + \omega\mathbf{C} + 2\jmath\omega^2\mathbf{M}$, e.g. see [34].

We now present numerical examples to illustrate properties of direct methods, i.e., methods based on a sparse LU factorization, and preconditioned Krylov solvers. Consider the numerical example from [33] with the 3D mesh shown in Figure 2.a. The matrix $\mathbf{K} - \omega^2\mathbf{M}$ is real symmetric and is of order 140,228 and has 1,822,668 nonzero elements. The LU factorization of $\mathbf{K} - \omega^2\mathbf{M}$ using MUMPS [38] on a Dell Latitude 6400 required 13 seconds in 2009. The construction of a Krylov basis of dimension 50 by the Lanczos method (excluding the LU factorization) required 15 seconds. This shows that the factorization cost is highly dominant. Consider another example from [34], which is a finite element problem with spherical infinite elements. The mesh is given in Figure 2.b. The system matrix in (11) is nonsymmetric and complex valued. The order is 72,976 and the matrix contains 1,541,904 nonzero elements. Timings on a Dell Latitude 6400 in 2009 showed that the direct solve with MUMPS required 119.13 seconds (LU factorization and forward and backward solve). BiCGStab with the ILU preconditioner from [34] required 52.20 seconds at frequency 200Hz and 103.71 seconds at 500Hz. It is well known that iterative methods perform typically badly for higher frequencies, which is confirmed by this experiment. We also see that direct methods are competitive with iterative ones for this problem.

In our experience, iterative methods are not competitive with direct methods for most applications in FE (vibro-)acoustic. Therefore, the use of a direct linear solver is very common in model order reduction. For a direct linear solver, the

highest cost is the sparse LU factorization. Once the LU factorization is performed, the solve cost is only a fraction, typically, 10% or less of the factorization cost. For this reason, the methods based on Krylov and rational Krylov sequences are very popular and by far the most efficient methods in terms of computational cost, since they reduce the number of matrix factorizations. In practice, it implies that methods, such as the dominant pole algorithm, the Iterative Rational Krylov Algorithm (IRKA), and variations on these methods are only used for models of relatively small scale. Unfortunately, Krylov methods usually lead to larger orders of the reduced order model for the same accuracy than balanced truncation or IRKA.

2.2 Frequency limitation

For model order reduction, one should be aware of the fact the mesh is only valid for a limited frequency range. This is another reason why (rational) Krylov methods are popular, as they focus on a limited interval on the $\jmath\omega$ axis. Sometimes, the high frequency eigenvalues of the discrete model are the most dominant ones, so that default implementations of methods such as the dominant pole algorithm, balanced truncation, and Iterative Rational Krylov (IRKA), cannot be used. However, there are modifications of these methods that limit the frequency range as well. For the dominant pole algorithm, it is sufficient to modify the definition of dominance, taking into account the frequency limitation [46]. For balanced truncation the frequency limitation can be taken into account: in [6], the right-hand-side of the Lyapunov equation is modified in such a way that the high frequency content is filtered out. However, the obtained ROM may no longer be stable.

2.3 Modal approximation

For the order reduction of mechanical models, modal approximation approaches have been very popular over the past decades both in research and engineering practice. These approaches are based on the practical observation that the response of a mechanical second order system is typically dominated by its lowest frequency modes. This is the result of the dynamics stiffness increasing considerably for higher frequency modes, resulting in small amplitude contributions to the overall response.

In its most basic version this approach uses a set of free-free eigenmodes $\mathbf{V}$ of the undamped model for the reduced order basis [21]:

$$\left(-\mathbf{M}_s\omega_i^2 + \mathbf{K}_s\right) V_i = 0, \quad \forall \omega_i \leq \omega_{max}, \tag{14}$$

where V_i is the modal shape vector at pulsation ω_i. An important benefit of this approach is the inherent inclusion of the limited frequency range in which the model discretization is valid. However, this basic approach tends to lead to poor accuracy as it does not account for the particular interface conditions of the model. In order to robustify with respect to these conditions, a range of extensions have been proposed which augment the initial modal basis with specific interface modes. The best known reduced order basis in this framework is the component mode synthesis (CMS) approach [13]. However, over the years many authors have proposed a range of approaches which fit this framework [9].

A major reason why these approaches tend to be popular in practice, is the clear physical interpretation of these ROMs. This if often important because practicing engineers tend to prefer approaches which they understand, as the ROM setup typically requires to tuning for different applications. However, these methods also suffer from two important drawbacks:

- No reliable error estimators exist for modal approximation approaches, leading to tedious tuning by the user to achieve the desired accuracy.
- The computation of the free-free modes can be an expensive for large scale models. This can limit the overall gains in the model evaluation time when also accounting for the MOR setup time.

As a result of these drawbacks, they are not discussed in more detail in the remainder of this chapter. Nevertheless, these modal reduction approaches are still very popular in practice. They moreover serve as inspiration for a range of novel nonlinear model order reduction schemes like the modal derivative approach for nonlinear problems, as discussed in Chapter Rixen.

2.4 Rational Krylov methods

For the sake of notation, let us repeat the idea of Krylov methods from Chapter Krylov methods and moment matching and their mathematical and algorithmic properties important for this chapter. Consider the following linear (descriptor) state-space model in the Laplace variable:

$$\begin{aligned} \mathbb{A}\mathbf{x} - s\mathbb{E}\mathbf{x} &= \mathbf{b} \\ H &= \mathbf{c}^T\mathbf{x} \end{aligned} \tag{15}$$

where $\mathbb{A}, \mathbb{E} \in \mathbb{R}^{\tilde{n}\times\tilde{n}}$, $\mathbf{b}, \mathbf{c} \in \mathbb{R}^{\tilde{n}}$ with $\tilde{n}$ large. (Rational) Krylov methods build a basis of dimension k, which we denote by matrix $\mathbf{V} \in \mathbb{C}^{\tilde{n}\times k}$, for the column space of

$$[\mathbf{K}_{m_1}((\mathbb{A}-\sigma_1\mathbb{E})^{-1}\mathbb{E}, (\mathbb{A}-\sigma_1\mathbb{E})^{-1}\mathbf{b}), \ldots, \mathbf{K}_{m_p}((\mathbb{A}-\sigma_p\mathbb{E})^{-1}\mathbb{E}, (\mathbb{A}-\sigma_p\mathbb{E})^{-1}\mathbf{b})].$$

with $\mathbf{K}_m(\mathbb{T}, \mathbf{b})$ the order m Krylov matrix

$$\mathbf{K}_m(\mathbb{T}, \mathbf{b}) = [\mathbf{b}, \mathbb{T}\mathbf{b}, \ldots, \mathbb{T}^{m-1}\mathbf{b}].$$

This sequence uses p different shifts, the jth shift with multiplicity m_j. Now let $\mathbf{W} \in \mathbb{C}^{n\times k}$ be an arbitrary rank k matrix. The order k reduced order model

$$\begin{aligned} \widehat{\mathbb{A}}\widehat{\mathbf{x}} - s\widehat{\mathbb{E}}\widehat{\mathbf{x}} &= \widehat{\mathbf{b}} \\ \widehat{H} &= \widehat{\mathbf{c}}^T\widehat{\mathbf{x}} \end{aligned} \tag{16}$$

with $\widehat{\mathbb{A}} = \mathbf{W}^T\mathbb{A}\mathbf{V}$, $\widehat{\mathbb{E}} = \mathbf{W}^T\mathbb{E}\mathbf{V} \in \mathbb{C}^{k\times k}$, and $\widehat{\mathbf{b}} = \mathbf{W}^T\mathbf{b}$, $\widehat{\mathbf{c}} = \mathbf{V}^T\mathbf{c} \in \mathbb{C}^k$, has the following moment matching properties:

$$\frac{d^j}{ds^j}\widehat{H}(\sigma_i) = \frac{d^j}{ds^j}H(\sigma_i), \quad j = 0, \ldots, m_i - 1, \quad i = 1, \ldots, p.$$

If, in addition, the columns of $\mathbf{W}$ span the adjoint space

$$[\mathbf{K}_{m_1}((\mathbb{A}-\sigma_1\mathbb{E})^{-T}\mathbb{E}^T, (\mathbb{A}-\sigma_1\mathbb{E})^{-T}\mathbf{c}), \ldots, \mathbf{K}_{m_p}((\mathbb{A}-\sigma_p\mathbb{E})^{-T}\mathbb{E}^T, (\mathbb{A}-\sigma_p\mathbb{E})^{-T}\mathbf{c})],$$

the reduced order model (16) has the following moment matching properties:

$$\frac{d^j}{ds^j}\widehat{H}(\sigma_i) = \frac{d^j}{ds^j}H(\sigma_i), \quad j = 0, \ldots, 2m_i - 1, \quad i = 1, \ldots, p.$$

The advantage of Krylov methods is that the poles can be chosen so that
1. the limitation to a frequency range is respected;
2. and the number of large scale LU-factorizations is small (in this case p).

The downside of the Iterative Rational Krylov Algorithm from Chapter Chapter IRKA and the Dominant Pole Algorithm from Chapter Dominant Pole Algorithm is the large computational cost due to a large number of sparse LU factorizations. In fact, if the number of factorizations is as large as the number of points required by a POD approach for the frequency axis, there is no interest in using such methods. Greedy methods (See Chapter Greedy Methods) do not guarantee the same approximation error as $\mathcal{H}_\infty$ and $\mathcal{H}_2$ minimization of the error, but they require less matrix factorizations.

The main disadvantage of a Krylov method is that, in general, stability is not guaranteed. We will see in §5 an application for which stability is guaranteed.

Another disadvantage is that the size of the reduced model may not be minimal for the same accuracy as balanced truncation. Krylov methods are popular because they produce a reasonably good reduction in a relatively low computational time for the reduced order model setup. As an extension, the obtained reduced order models can be further reduced by balanced truncation, e.g. [23], in order to mitigate the high setup cost of the balanced trunctation model on a high order model. We give other examples in §4.4.

2.5 Concept of linearization

The standard approach for mapping the second order matrix polynomial in (11) to a linear form is called linearization. Linearization allows to use model order reduction methods for linear models as in (15). Best known is the *companion linearization*. It doubles the dimension of the state space, but the system is linear and produces the same transfer function as the system with quadratic frequency dependency. System (11), with output $H = \mathbf{c}^T\mathbf{x}$, can be rewritten as the linear model

$$\begin{aligned} \left(\begin{bmatrix} \mathbf{K} & 0 \\ 0 & \mathbf{I} \end{bmatrix} + \jmath\omega \begin{bmatrix} \mathbf{C} & \mathbf{M} \\ -\mathbf{I} & 0 \end{bmatrix} \right) \begin{bmatrix} \mathbf{x} \\ \jmath\omega\mathbf{x} \end{bmatrix} &= \begin{bmatrix} \mathbf{f} \\ 0 \end{bmatrix} \\ H &= \begin{bmatrix} \mathbf{c} \\ 0 \end{bmatrix}^T \begin{bmatrix} \mathbf{x} \\ \jmath\omega\mathbf{x} \end{bmatrix}. \end{aligned} \tag{17}$$

Any method for linear systems can be used for reducing (17). It should be noted that the state vector now has two components: $\mathbf{x}$ and $\jmath\omega\mathbf{x}$. The Krylov vectors now have length $\tilde{n} = 2n$. However, due to the structure of the state space the memory cost of the iteration vectors can be halved [2].

Linearizations are also used for other polynomial, rational or even fully nonlinear dependencies on the frequency. Efficient implementations of Krylov methods (one and two sided) rely on a similar property as the state vector of second order problems, see [50] and [27]. We will give more examples in §4.

3 Structure preserving model order reduction

In many cases, it may be important to have a reduced order model that respects the structure of the large scale model. Such structures can take various forms: real matrices, symmetric matrices, polynomial frequency dependence and so on. For example, the typical structure for frequency domain vibration analysis is the form of (11). Finding a reduced order model of exactly the same structure (symmetric matrices, quadratic frequency dependence) may be beneficial for

keeping spectral properties, e.g., but also to physically interpret the reduced order model.

3.1 Quadratic frequency domain structure

In this section, we discuss the exploitation of quadratic structure as in (11). The choice of reduced order model depends on its purpose. If the model is to be coupled with other models in the time domain, a linear model is usually preferred, since the connection with the time domain is straightforward. For reliable time-domain simulation a stable model (which mechanical systems inherently are) is required, but this is not always the case for the ROM. By respecting the quadratic structure, the stability can sometimes be guaranteed.

For second order systems (11), Krylov methods rely on linearization (17). Assume that the reduced model is obtained by projection of (17) on subspace $\mathcal{V}$ spanned by the columns of the full rank matrix $\mathbf{V} \in \mathbb{C}^{2n\times k}$. Decompose

$$\mathbf{V} = \begin{bmatrix} \mathbf{V}_1 \\ \mathbf{V}_2 \end{bmatrix} \quad , \quad \mathbf{V}_1, \mathbf{V}_2 \in \mathbb{C}^{n\times k}.$$

Let $\mathbf{V}$ be computed by an interpolatory model order reduction method, i.e., a (rational) Krylov method, on (17). Interpolation at $\omega = \omega_i$ implies that $\mathbf{x}(\omega_i)$ is spanned by the columns of $\mathbf{V}_1$ and $\jmath\omega_i\mathbf{x}(\omega_i)$ by the columns of $\mathbf{V}_2$. This suggests that there is a strong connection between $\mathbf{V}_1$ and $\mathbf{V}_2$. Indeed, Second order Arnoldi (SOAR) [2], and Two-level Orthogonal Arnoldi (TOAR) [28], for example, exploit this property and express $\mathbf{V}_i = \mathbf{Q}\mathbf{U}_i$, $i = 1, 2$, with $\mathbf{Q} \in \mathbb{C}^{n\times\ell}$, $\mathbf{U}_i \in \mathbb{C}^{\ell\times k}$, where $\ell \leq k$. Instead of building a linear reduced model, one might, as in SOAR, compute a second order reduced model by projection on the column span of $\mathbf{Q}$:

$$\begin{aligned} (\widehat{\mathbf{K}} + \jmath\omega\widehat{\mathbf{C}} - \omega^2\widehat{\mathbf{M}})\widehat{\mathbf{x}} &= \widehat{\mathbf{f}} \\ \widehat{H} &= \widehat{\mathbf{c}}^T\widehat{\mathbf{x}} \end{aligned} \tag{18}$$

with $\widehat{\mathbf{K}} = \mathbf{Q}^T\mathbf{K}\mathbf{Q}$, $\widehat{\mathbf{C}} = \mathbf{Q}^T\mathbf{C}\mathbf{Q}$, $\widehat{\mathbf{M}} = \mathbf{Q}^T\mathbf{M}\mathbf{Q}$, $\widehat{\mathbf{f}} = \mathbf{Q}^T\mathbf{f}$, and $\widehat{\mathbf{c}} = \mathbf{Q}^T\mathbf{c}$.

The situation is more complicated for two-sided model order reduction. Indeed, the state vector of the adjoint of the linear problem

$$\begin{aligned} \begin{bmatrix} \mathbf{K}^T + \jmath\omega\mathbf{C}^T & -\jmath\omega\mathbf{I} \\ \jmath\omega\mathbf{M} & \mathbf{I} \end{bmatrix} \begin{bmatrix} \mathbf{z} \\ -\jmath\omega\mathbf{M}^T\mathbf{z} \end{bmatrix} &= \begin{bmatrix} \mathbf{c} \\ 0 \end{bmatrix} \\ H &= \begin{bmatrix} \mathbf{f} \\ 0 \end{bmatrix}^T \begin{pmatrix} \mathbf{z} \\ -\jmath\omega\mathbf{M}^T\mathbf{z} \end{pmatrix} \end{aligned} \tag{19}$$

has the two components $\mathbf{z} \in \mathbb{C}^n$ and $-\jmath\omega\mathbf{M}^T\mathbf{z} \in \mathbb{C}^n$. Now assume that the reduced model is obtained by projection on subspace $\mathcal{W}$ spanned by the columns

of the full rank matrix $\mathbf{W} \in \mathbb{C}^{2n\times k}$. Decompose

$$\mathbf{W} = \begin{bmatrix}\mathbf{W}_1\\ \mathbf{W}_2\end{bmatrix} \quad , \quad \mathbf{W}_1, \mathbf{W}_2 \in \mathbb{C}^{n\times k}.$$

Let $\mathbf{W}$ be computed by an interpolatory method on (19), i.e., there are ω so that $\mathbf{z}(\omega)$ is spanned by the columns of $\mathbf{W}_1$ and $\jmath\omega\mathbf{M}^T\mathbf{z}(\omega)$ by the columns of $\mathbf{W}_2$. This suggests that there is also a strong connection between $\mathbf{W}_1$ and $\mathbf{W}_2$. Indeed, in [27] this property is exploited by expressing $\mathbf{W}_1 = \mathbf{Z}\mathbf{T}_1$ and $\mathbf{W}_2 = \mathbf{M}^T\mathbf{Z}\mathbf{T}_2$ with $\mathbf{Z} \in \mathbb{C}^{n\times\ell}$, $\mathbf{T}_i \in \mathbb{C}^{\ell\times k}$, where $\ell \leq k$.

A linear reduced order model is obtained by projecting (17) on the right by $\mathbf{V}$ and the left by $\mathbf{W}^T$. A structure preserving alternative is to project (17) by

$$\begin{bmatrix}\mathbf{Q} & 0\\ 0 & \mathbf{Q}\end{bmatrix} \quad , \quad \begin{bmatrix}\mathbf{Z}^T & 0\\ 0 & \mathbf{Z}^T\mathbf{M}\end{bmatrix} \quad ,$$

on the right and the left, respectively. Note that the first spans the columns of $\mathbf{V}$ and the second the rows of $\mathbf{W}^T$, so, the interpolation properties are preserved with these bases. This leads to

$$\begin{bmatrix}\widehat{\mathbf{K}} + \jmath\omega\widehat{\mathbf{C}} & \jmath\omega\widehat{\mathbf{M}}\\ -\jmath\omega\widehat{\mathbf{M}} & \widehat{\mathbf{M}}\end{bmatrix}\begin{bmatrix}\hat{\mathbf{x}}\\ \jmath\omega\hat{\mathbf{x}}\end{bmatrix} = \begin{bmatrix}\widehat{\mathbf{f}}\\ 0\end{bmatrix}$$
$$\widehat{H} = \begin{bmatrix}\widehat{\mathbf{c}}\\ 0\end{bmatrix}^T\begin{bmatrix}\hat{\mathbf{x}}\\ \jmath\omega\hat{\mathbf{x}}\end{bmatrix},$$

with $\widehat{\mathbf{K}} = \mathbf{Z}^T\mathbf{K}\mathbf{Q}$, $\widehat{\mathbf{C}} = \mathbf{Z}^T\mathbf{C}\mathbf{Q}$, $\widehat{\mathbf{M}} = \mathbf{Z}^T\mathbf{M}\mathbf{Q}$, $\widehat{\mathbf{f}} = \mathbf{Z}^T\mathbf{f}$, and $\widehat{\mathbf{c}} = \mathbf{Q}^T\mathbf{c}$. Assuming that $\widehat{\mathbf{M}}$ has full rank, this is equivalent to the frequency-nonlinear model (18).

We now illustrate one sided linear and second order reduced models for the following example, whose description is taken from [58]. The model describes a footbridge located over the Dijle river in Mechelen (Belgium). It is about 31.354m in length and four tuned mass dampers (TMD) are located at nodes at 11.299m, 19.314m, 10.549m, and 20.309m, respectively, each of which weighs 40.72kg. The discretized model is

$$\left(\mathbf{K}_0 + \jmath\omega\mathbf{C}_0 + \sum_{i=1}^{4}\mathbf{K}_i - \omega^2\mathbf{M}_0\right)\mathbf{x} = \mathbf{f}$$

where $\mathbf{K}_0$ and $\mathbf{M}_0$ are obtained from a finite element model with $25,962$ DOFs, shown in Figure 3.a. Here, $\mathbf{C}_0 = 0.1003\mathbf{M}_0 + 0.0001591\mathbf{K}_0$ represents Rayleigh damping, $\mathbf{K}_i$ is a matrix with four nonzero entries that represents the interaction between the ith TMD and the footbridge, the input vector f represents an excitation equally spread among the locations of the TMDs. All matrices are

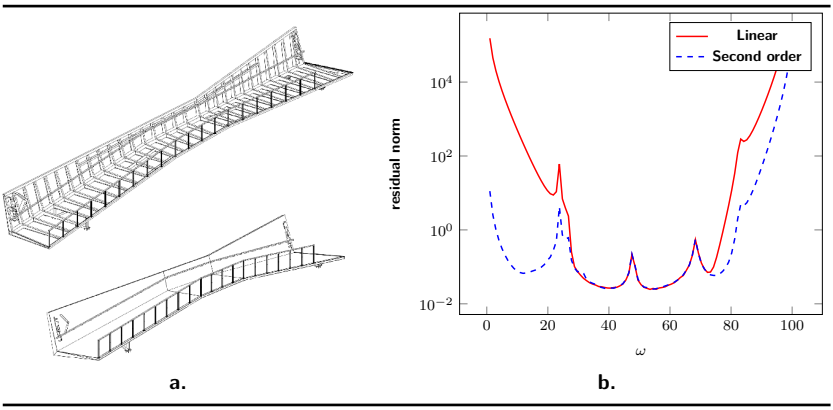


Fig. 3: a. Mesh. b. Residual norm on (11) for the linearized model and the original second order model

symmetric positive semi definite. We used twenty iterations of Arnoldi's method (Krylov method) with single shift $50.5\jmath$ on (17). A linear reduced order model was obtained by one sided projection $\widehat{\mathbb{A}} = \mathbf{V}^*\mathbb{A}\mathbf{V}$ and $\widehat{\mathbb{B}} = \mathbf{V}^*\mathbb{B}\mathbf{V}$ and a second order model of the form (18). Figure 3.b shows the residual norm of (11) for $\omega \in \jmath[0, 100]$ when (17) is projected on the Krylov space (linear model) and when (11) is projected on the column range of $\mathbf{Q}$ (second order model). It is easily seen that around the interpolation point, the error is of the same order of magnitude but that further away, the second order model has lower residual norms. This can be explained by the fact that projection of (11) is equivalent to projecting (17) on a larger subspace, similarly to two-sided models. An additional advantage for the second order model is that the matrices in (18) are Hermitian semi positive definite, so that stability of the reduced model is guaranteed. This is not the case for the linear reduced order model.

3.2 Lagrangian structure in mechanical models

For classical mechanical systems, the equations of motion in the form as presented in equation (10) can be obtained from a Lagrangian description of the system, with the Lagrangian $\mathcal{L}$:

$$\begin{aligned} \mathcal{L} &= \mathcal{K} - \mathcal{V} + \mathcal{W} \\ &= \frac{1}{2}\dot{\mathbf{x}}^T\mathbf{M}\dot{\mathbf{x}} - \frac{1}{2}\mathbf{x}^T\mathbf{K}\mathbf{x} - \mathbf{x}^T\mathbf{f}, \end{aligned} \tag{20}$$

where $\mathcal{K}$, $\mathcal{V}$, and $\mathcal{W}$ are respectively the kinetic energy, internal elastic energy and external work. The equations of motion are then obtained by applying Hamilton's principle to the Lagrangian:

$$\frac{d}{dt}\left(\frac{\partial \mathcal{L}}{\partial \dot{\mathbf{x}}}\right) - \frac{\partial \mathcal{L}}{\partial \mathbf{x}} = \mathbf{f}. \tag{21}$$

This Lagrangian structure inherently embeds energy preserving behavior in the system, ensuring stability for long term simulations. It is therefore important that the reduced order models for mechanical systems respect this structure. In order to ensure that the resulting ROM equations of motion comply with this Lagrangian structure, a direct substitution in the Lagrangian can be performed. For a constant reduced order basis, on can substitute for the reduced DOFs q:

$$\mathbf{x} \simeq \mathbf{V}\mathbf{q}, \qquad \dot{\mathbf{x}} \simeq \mathbf{V}\dot{\mathbf{q}}, \tag{22}$$

which results in the Lagrangian expressed as a function of the reduced order DOFs $\mathbf{q}$:

$$\mathcal{L} = \frac{1}{2}\dot{\mathbf{q}}^T\mathbf{V}^T\mathbf{M}\mathbf{V}\dot{\mathbf{q}} - \frac{1}{2}\mathbf{q}^T\mathbf{V}^T\mathbf{K}\mathbf{V}\mathbf{q} - \mathbf{q}^T\mathbf{V}^T\mathbf{f}, \tag{23}$$

such that after application of Hamilton's principle for the reduced DOFs, the reduced equations of motion become:

$$\mathbf{V}^T\mathbf{M}\mathbf{V}\ddot{\mathbf{q}} + \mathbf{V}^T\mathbf{K}\mathbf{V}\mathbf{q} = \mathbf{V}^T\mathbf{f}. \tag{24}$$

As this form results from the (reduced) Lagrangian of the system, it inherently preserves the stability of the underlying mechanical model.

This implies some care on how the model order reduction on a mechanical system is applied, as the models are often presented in different form. For example, for practical time domain simulations, equation (10) is often converted to a first order state-space model as:

$$\begin{bmatrix}\dot{\mathbf{x}}\\ \ddot{\mathbf{x}}\end{bmatrix} = \begin{bmatrix}0 & \mathbf{I}\\ -\mathbf{M}^{-1}\mathbf{K} & 0\end{bmatrix}\begin{bmatrix}\mathbf{x}\\ \dot{\mathbf{x}}\end{bmatrix} + \begin{bmatrix}0\\ \mathbf{f}\end{bmatrix}. \tag{25}$$

In a regular projection framework, state-space system (25) would be reduced as:

$$\begin{bmatrix}\mathbf{x}\\ \dot{\mathbf{x}}\end{bmatrix} = \mathbf{V}\mathbf{q} = \begin{bmatrix}\mathbf{V}_1\\ \mathbf{V}_2\end{bmatrix}\mathbf{q}, \quad \mathbf{V}^T\mathbf{V} = \mathbf{I} \tag{26}$$

and one would obtain a reduced system of equations as:

$$\dot{\mathbf{q}} = \begin{bmatrix}0 & \mathbf{V}_1^T\mathbf{I}\mathbf{V}_2\\ -\mathbf{V}_2^T\mathbf{M}^{-1}\mathbf{K}\mathbf{V}_1 & 0\end{bmatrix}\mathbf{q} + \begin{bmatrix}0\\ \mathbf{V}_2^T\mathbf{f}\end{bmatrix}. \tag{27}$$

It is now clear that this system of equations cannot be converted back into a Lagrangian form like (23), such that time stable and energy preserving behavior is not naturally preserved. From this perspective, it is advisable to always apply symmetric projection of the second order system for mechanical models if the ROM will be employed in time-domain simulations. This again shows the conceptual benefit of approaching mechanical reduced order models through a one-sided projection on the second order system.

4 Complex frequency dependencies

4.1 Sources of nonlinearities

To mitigate noise and vibration issues in mechanical engineering applications, damping treatments are often applied. The physical behavior of these treatments are mostly represented by (complex) frequency-dependent behaviour. Poro-elastic materials, for example, are often used in a sound absorption context. An overview of modeling approaches for poro-elastic materials can be found in amongst others [1, 14]. Visco-elastic materials are often applied in a constrained component setting as this ensures shear, and thus more dissipation in the sample. Their behaviour strongly depends on temperature and frequency. A detailed description of various mathematical models are given in [17, 43].

When unbounded acoustic domains are considered (exterior problems), using Finite Element models, the domain has to be truncated in practice. In this case the Sommerfeld radiation condition [11], which ensures that no acoustic energy reflects back from infinity, has to be approximated. Commonly applied approaches, like absorbing boundary conditions [3] and perfectly matched layers [8] also result in complex frequency dependencies.

4.2 Rational and polynomial frequency dependencies

We assume that the frequency dependent full order system, of order n, can be written as:

$$\begin{aligned} \mathbb{A}(s)\mathbf{x} &= \mathbf{f} \\ H &= \mathbf{c}^T\mathbf{x} \\ \text{with} \quad \mathbb{A}(s) &= \sum_{i=0}^{d-1} \phi_i(\mathbb{A}_i + s\mathbb{B}_i) \quad \text{and} \quad s = \jmath\omega\,. \end{aligned} \tag{28}$$

We introduce the following notation:

$$\begin{aligned} \mathbf{A} + s\mathbf{B} &= [\mathbb{A}_0 + s\mathbb{B}_0, \ldots, \mathbb{A}_{d-1} + s\mathbb{B}_{d-1}], \\ \mathbf{\Phi} &= [\phi_0, \ldots, \phi_{d-1}]^T\,. \end{aligned}$$

where $\mathbf{\Phi}$ forms a set of polynomials or rational polynomials that satisfy:

$$(\mathbf{P} + s\mathbf{R})\mathbf{\Phi} = 0$$

with $\mathbf{P}, \mathbf{R} \in \mathbb{C}^{(d-1)\times d}$ constant matrices. This leads to:

$$\mathbb{A}(s) \quad = \quad (\mathbf{A} + s\mathbf{B})(\mathbf{\Phi} \otimes \mathbf{I}_n)\,.$$

As a result (28) can be rewritten as an order nd linear system:

$$\begin{bmatrix} \mathbf{A} + s\mathbf{B} \\ (\mathbf{P} + s\mathbf{R}) \otimes \mathbf{I}_n \end{bmatrix} \begin{pmatrix} \phi_0\mathbf{x} \\ \phi_1\mathbf{x} \\ \vdots \\ \phi_{d-1}\mathbf{x} \end{pmatrix} \quad = \quad \begin{pmatrix} \mathbf{f} \\ 0 \\ \vdots \\ 0 \end{pmatrix}$$

$$H \quad = \quad [\mathbf{c}^T \; 0 \; \cdots \; 0] \begin{pmatrix} \phi_0\mathbf{x} \\ \vdots \\ \phi_{d-1}\mathbf{x} \end{pmatrix}$$

or in compact form:

$$\begin{bmatrix} \mathbf{A} + s\mathbf{B} \\ (\mathbf{P} + s\mathbf{R}) \otimes \mathbf{I}_n \end{bmatrix} (\mathbf{\Phi} \otimes x) \quad = \quad e_1 \otimes \mathbf{f} \tag{29}$$

$$H \quad = \quad (e_1 \otimes \mathbf{c})^T (\mathbf{\Phi} \otimes \mathbf{x})$$

which is clearly linear in s. For the companion linearization from §2.5 of second order problems, $\mathbf{R} = [-1, 0]$, $\mathbf{P} = [0, 1]$, $\mathbf{\Phi}(s) = [1, s]^T$. For the rational matrix polynomial:

$$\mathbb{A}(s) = (\mathbb{A}_0 + s\mathbb{B}_0) + \frac{1}{s - \sigma_0}(\mathbb{A}_1 + s\mathbb{B}_1) + \frac{1}{s - \sigma_1}(\mathbb{A}_2 + s\mathbb{B}_2),$$

a possible linearization is:

$$\begin{bmatrix} \mathbb{A}_0 + s\mathbb{B}_0 & \mathbb{A}_1 + s\mathbb{B}_1 & \mathbb{A}_2 + s\mathbb{B}_2 \\ \mathbf{I} & \sigma_0\mathbf{I} - s\mathbf{I} & 0 \\ \mathbf{I} & 0 & \sigma_1\mathbf{I} - s\mathbf{I} \end{bmatrix} \begin{pmatrix} \mathbf{x} \\ \frac{1}{s-\sigma_0}\mathbf{x} \\ \frac{1}{s-\sigma_1}\mathbf{x} \end{pmatrix} = \begin{pmatrix} \mathbf{f} \\ 0 \\ 0 \end{pmatrix}.$$

In this case, the choice of basis and the choice of linearization is important. Some formulations lead to a descriptor system, which may require additional care for proper setup of the ROM. However, for models in the frequency domain, we have never experienced difficulties in this case.

It can be proven that the (rational) Arnoldi method for (29) produces iteration vectors that take the following form: if the k vectors are collected in an $nd \times k$ matrix $\mathbf{V}_k$, this matrix can be factored as

$$\mathbf{V}_k = (\mathbf{I}_d \otimes \mathbf{Q})\mathbf{U}_k \quad , \quad \mathbf{Q} \in \mathbb{C}^{n\times\ell}, \mathbf{U} \in \mathbb{C}^{\ell d\times k}, \tag{30}$$

with $\ell \leq k + d$ [28] [50]. The advantage of this factorization is that large scale operations only happen with columns of $\mathbf{Q}$ and that all other operations are small scale. This leads to a reduction of the full unstructured storage of Krylov vectors of order ndk to at most $n\ell + \ell dk$ with $\ell \leq k + d$ [50]. For two-sided Krylov methods, the exploitation of the structure of (29) is possible, but, is more involved [40] [19] [27]. In each iteration of a Krylov method, a linear system is solved. In [50], it is shown that this requires matrix vector multiplications with $\mathbb{A}_i$ and $\mathbb{B}_i$ and a linear solve with $\mathbb{A}(\sigma_k)$ at step k.

As for second order problems, $\mathbf{Q}$ can be used to develop a nonlinear frequency dependent reduced model:

$$\widehat{\mathbb{A}} = \sum_{j=0}^{d-1} (\widehat{\mathbb{A}}_j + s\widehat{\mathbb{B}}_j)\phi_j, \quad \widehat{\mathbb{A}}_j + s\widehat{\mathbb{B}}_j = \mathbf{Q}^*(\mathbb{A}_j + s\mathbb{B}_j)\mathbf{Q}, \quad j = 0, \ldots, d-1.$$

If all shifts $\sigma_1, \ldots, \sigma_k$ are distinct, then

$$\text{Range}(\mathbf{Q}) = \text{Range}([\mathbf{x}(\sigma_1), \ldots, \mathbf{x}(\sigma_k)]) = \text{Range}([\mathbb{A}(\sigma_1)^{-1}\mathbf{f}, \ldots, \mathbb{A}(\sigma_k)^{-1}\mathbf{f}]). \tag{31}$$

When the shifts are all equal,

$$\text{Range}(\mathbf{Q}) = \text{Range}([\mathbf{x}(\sigma_1), d\mathbf{x}(\sigma_1)/ds, \ldots, d^{k-1}\mathbf{x}(\sigma_1)/ds^{k-1}]). \tag{32}$$

In other words, the range of $\mathbf{Q}$ spans the moments of the state vector $\mathbf{x}$ of (28). If only $\mathbf{Q}$ is required, a linearization is not useful, since $\mathbf{Q}$ can be computed directly using (31) or (32), which requires linear solves with $\mathbb{A}(s)$. However, in the case of higher order interpolation, as in (32), the computation of the derivatives is equally complicated as performing a Krylov step with the linearization.

If a linear reduced order model is required, then a linearization is useful. In this case, (29) is projected using the full Krylov vectors given by the factorization (30). For two-sided model order reduction, with simple interpolation points, a linear reduced model can equally be obtained by putting samples of H from (28) in a Loewner matrix [32]. In this case, the reduced model is defined with:

$$\widehat{\mathbb{E}} = \begin{bmatrix} \frac{H(\sigma_1)-H(\tau_1)}{\sigma_1-\tau_1} & \cdots & \frac{H(\sigma_k)-H(\tau_1)}{\sigma_k-\tau_1} \\ \vdots & \ddots & \vdots \\ \frac{H(\sigma_1)-H(\tau_k)}{\sigma_1-\tau_k} & \cdots & \frac{H(\sigma_k)-H(\tau_k)}{\sigma_k-\tau_k} \end{bmatrix}$$

$$\widehat{\mathbb{A}} = \begin{bmatrix} \frac{\sigma_1 H(\sigma_1)-\tau_1 H(\tau_1)}{\sigma_1-\tau_1} & \cdots & \frac{\sigma_k H(\sigma_k)-\tau_1 H(\tau_1)}{\sigma_k-\tau_1} \\ \vdots & \ddots & \vdots \\ \frac{\sigma_1 H(\sigma_1)-\tau_k H(\tau_k)}{\sigma_1-\tau_k} & \cdots & \frac{\sigma_k H(\sigma_k)-\tau_k H(\tau_k)}{\sigma_k-\tau_k} \end{bmatrix},$$

and

$$\widehat{\mathbf{b}} = \begin{bmatrix} H(\sigma_1) \\ H(\sigma_2) \\ \vdots \\ H(\sigma_k) \end{bmatrix}, \quad \widehat{\mathbf{c}} = \begin{bmatrix} \bar{H}(\tau_1) \\ \bar{H}(\tau_2) \\ \vdots \\ \bar{H}(\tau_k) \end{bmatrix}.$$

When the interpolation points are not too close to each other, this is a reliable and easy to implement method.

We now present two cases of nonlinear frequency dependency. The first case, presented in §4.3, uses (31) to directly construct $\mathbf{Q}$ and computes a linear reduced order model using Loewner matrices. The second case uses (32) to reduce the number of matrix factorizations; see §4.4.

4.3 Matrix free Model Order Reduction for vibro-acoustic systems with complex noise control treatments

Many model order reduction methods cannot straightforwardly cope with frequency dependencies in vibro-acoustic models, resulting from, amongst others, complex damping treatments or infinite acoustic domains. In this section, a matrix-free Krylov MOR method [24] is presented that does not require knowledge on the underlying mathematical model and that can straightforwardly handle problems with frequency dependent parameters in exactly the same manner as problems with constant properties. The method only works in the frequency domain and is based on two-sided model order reduction approach with distinct interpolation points using the Loewner matrices as discussed in Section 4.2. The frequency dependent transfer function between input and output is indicated by $H(\omega)$. The use of the Loewner matrices leads to a new approximative transfer function $\hat{H}$ which interpolates the original transfer function H, using the forced responses at the $2k$ distinct interpolation points.

4.3.1 Frequency selection and convergence evaluation

In the following, let $\hat{H}_k$ denote the transfer function (or frequency response function) obtained using a Loewner model of order k, i.e., using k right interpolation points and k left interpolation points. Jonckheere *et al.* [44, 45] present two criteria to assess the convergence of the reduced order model, which leads to a greedy method for determining the interpolation points. The first convergence criterion is based on the relative error between two subsequent ROM approximations, which is computationally cheap to evaluate:

$$\varepsilon_{\text{ROM,ROM}} = \max_{\omega} \left| \frac{\hat{H}_k(\omega) - \hat{H}_{k-1}(\omega)}{\hat{H}_k(\omega)} \right|. \tag{33}$$

However, the relative error between two subsequent approximations may be low in case the newly added frequencies are close to the frequencies added in the previous iteration and bring limited additional information to the interpolation. Therefore, a second convergence criterion is embedded by comparing the (approximated) transfer function obtained using the current ROM with the (exact) transfer function, calculated by solving the full system, at the newly selected frequency lines ω_k which would be needed to build a new ROM in the next iteration:

$$\varepsilon_{\text{ROM,Full}} = \max_{\omega_k} \left| \frac{\hat{H}_k(\omega) - H_k(\omega)}{\hat{H}_k(\omega)} \right| . \tag{34}$$

The relative error between two subsequent ROMs (33) is used to select new frequency lines to enrich the ROM in the next iteration. This selection is done in a cascading way: (i) the frequency at which the maximum error occurs is selected, (ii) the direct vicinity of the new frequency line is masked to avoid selecting neighbouring maxima, thus to spread out the new frequency lines a bit, (iii) from the remaining frequencies the one corresponding to the new maximum error is selected and the procedure continues along (ii)-(iii) until the requested number of additional frequency lines is reached.

4.3.2 Calculation example

One example considering a mechanical system with complex damping treatments, taken from [44] is presented. The example geometry is shown in Figure 4, which is taken from the Comsol manual [37]. This interior car cavity has dimensions of approximately 4.5m by 1.5m by 2m and has 26 acoustic modes below 300Hz. All acoustic boundaries are rigid, except for the fire wall (indicated in light blue) where an acoustic acceleration of 1 m/s^2 is imposed. The density of air is specified as 1.2 kg/m^3 and the speed of sound as 343.8 m/s. On the seats a frequency dependent impedance is applied, where the impedance is calculated from tabulated values of absorption coefficients. The acoustic pressure is tracked at the driver's ear as output quantity. The finite element model consists of 1372332 DOFs. The calculation of a single frequency line took approximately 69.5s for the damped case on a Linux Cluster, using two 10-core Ivy Bridge Xeon E5-2680v2 CPUs (2.8 GHz, 128 GB RAM). The frequency range from 1 to 300Hz is simulated with a 1 Hz step to set up the reference data.

For this example, the starting point is a steady-state dynamic equation of the form:

$$[\mathbf{K}(\omega) - \omega^2 \mathbf{M}(\omega)]\mathbf{x} = \mathbf{f}, \tag{35}$$

where $\mathbf{M}, \mathbf{K} \in \mathbb{R}^{n \times n}$ are in this case frequency dependent complex mass and stiffness matrices accounting for damping effects. Notice that, in this case, $s = (\jmath\omega)^2$ in contrast to §4.2.

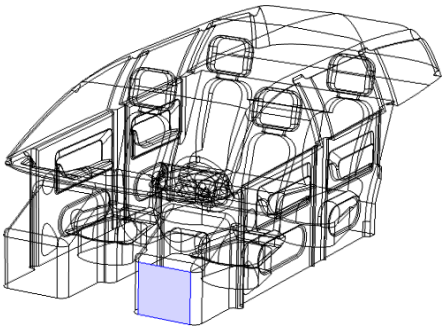


Fig. 4: Car cavity geometry with porous seats with complex frequency dependent behavior

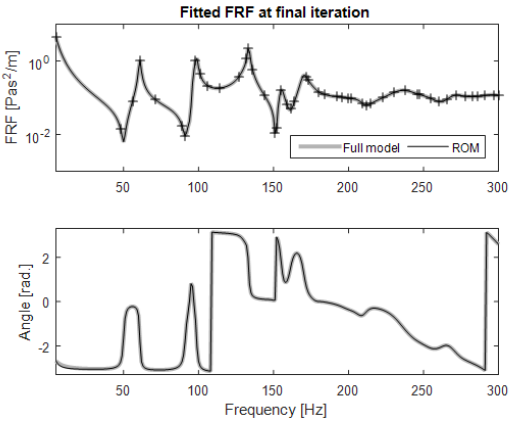


Fig. 5: Acoustic frequency response function for car cavity with porous seats, final approximation for the acceleration transfer function, crosses indicate the interpolation frequencies

Figure 5 shows the original and the fitted frequency response functions. The matrix-free approach starts with an initial calculation of two frequency lines, setting the boundaries of the frequency range of interest (5Hz and 300Hz). Thereafter, two additional frequency lines are computed and used to build a new ROM. When the requested accuracy of 1% is met, both on $\varepsilon_{ROM,ROM}$ and $\varepsilon_{ROM,Full}$, the algorithm terminates (after 24 iterations, requiring only 48 frequency evaluations). A speed-up factor of 6 is obtained for the acoustic frequency response assessment in this particular case.

4.4 Rational approximation

When $\mathbb{A}(s)$ is generally nonlinear, i.e., not polynomial or rational, linearizations can still be used on polynomial or rational approximations. Rational approximation, in particular, is very powerful as we will now illustrate. The idea presented here is to approximate $\mathbb{A}(s)$ by a rational polynomial with d terms as in (28). Over the years, a number of approaches have been developed to perform these approximations. In [57], a Taylor expansion is used. In [49] and [47], $\mathbb{A}(s)$ is approximated by a truncated Padé series. In [47], windowing is used to cover the entire frequency range, and in [36], a spectral discretization is used. In [26], a rational approximation based on the Adaptive Antoulas Anderson method, also known as AAA and pronounced as 'Triple A' is proposed.

Here, we will present the idea from [26], since it is an elegant and user friendly way to find a rational approximation for the model. For the implementation details, we refer to [26]. Assume that $\mathbb{A}$ has the following form:

$$\mathbb{A}(s) = \mathbf{K} + s\mathbf{C} + s^2\mathbf{M} + \sum_{p=1}^{m} (\mathbb{A}_p + s\mathbb{B}_p) f_p(s)$$

with $f_p : \mathbb{C} \to \mathbb{C}$ a scalar function in s. First, the general nonlinearity is approximated by a rational function, expressed in barycentric rational form [39]. After the approximation, the matrix can be written as the rational matrix polynomial:

$$\mathbb{A}(s) \simeq \mathbf{K} + s\mathbf{C} + s^2\mathbf{M} + \sum_{i=0}^{d-1} \left(\sum_{p=1}^{m} (\mathbb{A}_p + s\mathbb{B}_p) f_p(\zeta_i) \right) \frac{\omega_i/(\jmath\omega - \zeta_i)}{\sum_{k=0}^{d-1} \omega_k/(\jmath\omega - \zeta_k)},$$

where ω_i, for $i = 0, \ldots, d-1$ are called the weights and ζ_i the support points. The AAA method chooses d, ω_i, ζ_i for $i = 0, \ldots, d-1$ so that:

$$\sup_{\omega \in [\omega_{\min}, \omega_{\max}]} \left| f_p(\jmath\omega) - \sum_{i=0}^{d-1} f_p(\zeta_i)) \frac{\omega_i/(\jmath\omega - \zeta_i)}{\sum_{k=0}^{d-1} \omega_k/(\jmath\omega - \zeta_k)} \right|, \tag{36}$$

is below a given tolerance for $p = 1, \ldots, m$. The AAA method determines the parameters automatically in very little time. Only the function values of f_p for the test set are required. There is no need to compute derivatives. The criterion (36) is discretized in a number of points on the frequency axis. The support points ζ_i are chosen using a greedy method. The minimization of the residual leads to the weights ω_i.

The following example is based on a system from [22][35]. The results are reported in [25]. For this example, we consider the following time delay differential

equation:

$$\frac{\partial v}{\partial t} = \nabla^2 v + \sum_{j=1}^{3} a_j v + bu,$$
$$q = \langle c, v \rangle,$$

We set the domain to $[0, \pi] \times [0, \pi] \times [0, \pi]$, and let

$$\begin{aligned} a_1(x, y, z) &= 2\sin(\pi - x)\sin(y)\sin(z), \\ a_2(x, y, z) &= 2\sin(x)\sin(\pi - y)\sin(z), \\ a_3(x, y, z) &= 2\sin(x)\sin(y)\sin(\pi - z), \end{aligned}$$

and $\tau_1 = 1, \tau_2 = 2, \tau_3 = 4$. For the domain discretization we use central differences with N discretization points in each spatial variable. After transforming to the frequency domain, we get:

$$\begin{cases} \left(\mathbb{A}_0 - sI + \sum_{j=1}^{m} \mathbb{A}_j e^{-\tau_j s} \right) \mathbf{x}(s) = -\mathbf{b}u(s), \\ H(s) = \mathbf{c}^* x(s), \end{cases} \tag{37}$$

where $s = \jmath\omega =$, $\mathbb{A}_j \in \mathbb{R}^{n \times n}$, $\mathbf{x}, \mathbf{b}, \mathbf{c} \in \mathbb{R}^n$ and $n = N^3$. We are interested in solutions in the range $\omega \in [0.01, 10]$. The resulting system matrices are symmetric. Furthermore, the input application vector $\mathbf{b}$ is chosen as a vector containing random values in $[0, 1]$ and $\mathbf{c} = \mathbf{b}$. In the following, we show the relative error of the transfer function:

$$\epsilon(s) = \frac{|\widehat{H}(s) - H(s)|}{|H(s)|},$$

with

$$H(s) = \mathbf{c}^* \mathbb{A}(s)^{-1} \mathbf{b}, \quad \text{and} \quad \widehat{H}(s) = \widehat{\mathbf{c}}^* \left(\widehat{\mathbb{A}} - s\widehat{\mathbb{E}} \right)^{-1} \widehat{\mathbf{b}}.$$

The error is computed over the test set ω_j, $j = 1, \ldots, 500$, with logarithmically spaced points in the interval $[10^{-2}, 10]$, as values closer to zero are of particular interest.

For the AAA approximation, a test set of size 10000 is chosen over the interval $[0.01, 10]$. The AAA algorithm results in an approximation of the three non-linear functions with $d = 22$.

We now compare the results of three numerical methods:

RKS A rational Krylov sequence of order $K = 150$ obtained by using the three shifts $0\jmath, 5\jmath, 10\jmath$, each one fifty times. This leads to a linear reduced model.

LÖW A linear reduced model using Loewner matrices is used of order $k = 40$ with equidistant interpolation points in $[0.01\jmath, 10\jmath]$.

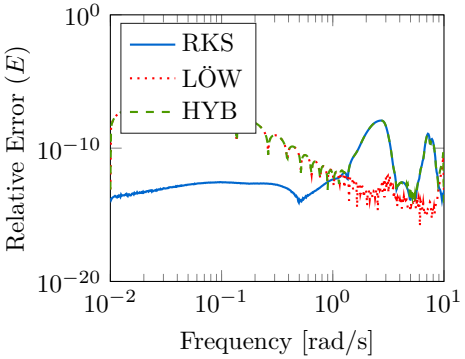


Fig. 6: Relative error as a function of the frequency $f = \mathrm{Re}(s)$ for $n = 30$. Linear pencil of reduced dimension $K = 150$ (——), Loewner with $k = 40$ (·····) and IRKA applied to the reduced pencil with $k = 40$ (- - -).

HYB A hybrid approach where the reduced model of order $K = 150$ from RKS is further reduced to order $k = 40$ by applying LÖW.

For $N = 40$, i.e., $n = 64,000$, the relative error for RKS of size $K = 150$, for LÖW for $k = 40$, and for HYB is plotted in Figure 6. From the figure, it is clear that the Loewner pencil leads to a lower reduced dimension for the same error level in the higher frequency range. The hybrid approach produces a model of size 40 with an error that is the maximum of the errors of RKS and LÖW. The difference between Loewner and hybrid appraoch lies in the execution time. For the Loewner approach, the simple interpolation using Loewner matrices required eighty large sparse matrix factorizations, where, for the rational Krylov and hybrid approaches only three matrix factorizations are performed. The cost of the Loewner approximation on the model of order 150 in the hybrid approach is therefore negligible. The computations were timed, averaged over three runs, on a machine with 64-bit Intel processor, 28 cores, 2.6 Ghz processors and 128 GB RAM. The hybrid approach required 384.7 seconds, where Loewner approach required 1814.9 seconds, which is a significant factor of 4.7 of the computation time for the hybrid approach.

A second example is described in [26]. This model was generated using a mesh from a Siemens Industry Software and applying poro-elastic material properties. The following matrix-valued function describes the nonlinear behaviour of the sound pressure inside a car cavity with porous seats, represented by a Johnson-Champoux-Allard equivalent fluid model [1]:

$$\mathbb{A}(\omega) = \mathbf{K}_0 + h_K(\omega)\mathbf{K}_1 - \omega^2(\mathbf{M}_0 + h_M(\omega)\mathbf{M}_1),$$

Table 1: Constants of the car cavity model

α_∞	1.7	σ	$13500 kg m^{-3} s^{-1}$	ϕ	0.98
η	$1.839 \cdot 10^{-5}$	Λ	$80 \cdot 10^{-6} m$	Λ'	$160 \cdot 10^{-6} m$
γ	1.4	ρ_0	1.213	P_r	0.7217

where $\mathbf{K}_0, \mathbf{K}_1, \mathbf{M}_0, \mathbf{M}_1 \in \mathbb{R}^{n \times n}$ with $n = 15036$ are symmetric, positive semidefinite matrices and ω is the angular frequency. The nonlinear functions are given by

$$h_K(\omega) = \frac{\phi}{\alpha(\omega)}, \quad \alpha(\omega) = \alpha_\infty + \frac{\sigma\phi}{i\omega\rho_0}\sqrt{1 + i\omega\rho_0 \frac{4\alpha_\infty^2 \eta}{\sigma^2 \Lambda^2 \phi^2}},$$

and

$$h_M(\omega) = \phi\left(\gamma - \frac{\gamma - 1}{\alpha'(\omega)}\right), \quad \alpha'(\omega) = 1 + \frac{8\eta}{i\omega\rho_0\Lambda'^2 P_r}\sqrt{1 + i\omega\rho_0 \frac{\Lambda'^2 P_r}{16\eta}},$$

with the parameters defined in Table 1.

The AAA approximation was built by approximating h_K and h_M in the ω range $[50, 1000\pi]$. This led to a rational approximation with 12 support points with a relative error of 10^{-12} for both functions on this interval. Six shifts, namely $1595.8\jmath$, $2173.92\jmath$, $2742.78\jmath$, $1125.87\jmath$, $3039.57\jmath$, and $50\jmath$, were selected using a greedy approach on the linear system's residual norm, where 20 Krylov iterations were performed for each shift. The dimension 120 was further reduced by applying POD in the frequency domain on this model to obtain an order of 77 for a relative tolerance of 10^{-8}.

5 Vibro-acoustic model order reduction

5.1 Stability-preserving model order reduction for vibro-acoustics

For coupled vibro-acoustic problems, the advantages of MOR have been demonstrated in literature in the frequency domain, see e.g. [20, 42]. However, popular reduced order techniques for frequency domain analysis cannot directly be applied to time domain analysis as these techniques do not necessarily preserve the stability of the original system [7]. While this loss of stability has no negative consequences on the frequency domain analysis of the vibro-acoustic system, it may lead to a diverging response in the time domain.

5.1.1 Conditions for stability of a linear descriptor system in a one-sided projection

In [52] general conditions are derived that ensure to preserve the stability of a linear descriptor system in a one-sided projection. The semi-discretized system model in the time domain:

$$\begin{aligned} \mathbb{E}\dot{\mathbf{x}}(t) &= \mathbb{A}\mathbf{x}(t) + \mathbf{b}\mathbf{u}(t) \\ H(t) &= \mathbf{c}^T\mathbf{x}(t)\,, \end{aligned} \tag{38}$$

is critically stable if all of the generalised eigenvalues of the matrix pair $\{\mathbb{A}, \mathbb{E}\}$ have a negative real part [15]. It is proven that stability is preserved in the one-sided projection of the descriptor system in (38) if $\mathbb{E} = \mathbb{E}^T$ and if $\mathbb{E}$ is positive-definite and if $\mathbb{A}$ is negative semi-definite. A matrix $\mathbf{Q} \in \mathbb{R}^{n\times n}$ is positive semi-definite if

$$\mathbf{x}^T\mathbf{Q}\mathbf{x} \geq 0$$

for any non-zero vector $\mathbf{x} \in \mathbb{R}^n$.

5.1.2 $u-p$ formulation and modified $u-\phi$ formulation

The vibro-acoustic model is generally described by (12), but depending on the exact formulation used for the model, different coupling matrices are present. Through a Galerkin approach for the FE model for the acoustic problem, it follows that the acoustic system matrices $\mathbf{K}_a$, $\mathbf{M}_a$, and $\mathbf{C}_a$ are all symmetric positive (semi-)definite. Typically, $\mathbf{M}_a$ is of full rank, which makes it strictly positive definite. Whether $\mathbf{K}_a$ is strictly or semi-positive definite depends on the boundary conditions. Similar conclusions can be drawn for the structural FE model and the corresponding system matrices $\mathbf{K}_s$, $\mathbf{M}_s$, and $\mathbf{C}_s$.

In case $\mathbf{K}_a$ and $\mathbf{K}_s$ are positive semi-definite, the zero eigenvalues of these matrices correspond to rigid body modes of the system, manifesting themselves as system poles at the origin of the complex plane. These poles do not adversely affect the stability of the system and are disregarded in the subsequent analysis without loss of generality. This implies that we can consider $\mathbf{K}_s$ and $\mathbf{K}_a$ to be strictly positive definite.

In [52] the definiteness of the global system matrices of the coupled vibro-acoustic finite element model, eq. (13) are investigated. While the coupled damping matrix $\mathbf{C}_{up}$ is positive (semi-)definite, $\mathbf{K}_{up}$ and $\mathbf{M}_{up}$ are generally not positive definite due to the presence of $\mathbf{K}_c$ and $\mathbf{M}_c$. Consequently, also $\mathbb{E}_{up}$ and $\mathbb{A}_{up}$ of the equivalent descriptor system (38) are indefinite as well. Even though

the vibro-acoustic system itself is stable, this stability is possibly lost in a regular one-sided projection.

Everstine [16] proposes an alternative, symmetric formulation for the vibro-acoustic problem which uses the scalar fluid velocity potential ϕ instead of the pressure p to describe the state of the fluid part of the vibro-acoustic system. This fluid velocity potential is defined by

$$p = -\rho\dot{\phi}\,, \tag{39}$$

with fluid density ρ, such that the vector containing the nodal pressure values in the fluid can be expressed as $\mathbf{p} = -\rho\dot{\boldsymbol{\phi}}$. The use of this $u-\phi$ formulation results in the symmetric system of equations which can be constructed from the $u-p$ model matrices:

$$\mathbf{M}_{u\phi}\ddot{\mathbf{x}}_{u\phi} + \mathbf{C}_{u\phi}\dot{\mathbf{x}}_{u\phi} + \mathbf{K}_{u\phi}\mathbf{x}_{u\phi} = \mathbf{f}_{u\phi}\,, \tag{40}$$

with

$$\mathbf{M}_{u\phi} = \begin{bmatrix} \mathbf{M}_s & 0 \\ 0 & -\rho\mathbf{M}_a \end{bmatrix} \qquad \mathbf{C}_{u\phi} = \begin{bmatrix} \mathbf{C}_s & -\rho\mathbf{K}_c \\ -\rho\mathbf{K}_c^T & -\rho\mathbf{C}_a \end{bmatrix} \qquad \mathbf{K}_{u\phi} = \begin{bmatrix} \mathbf{K}_s & 0 \\ 0 & -\rho\mathbf{K}_a \end{bmatrix}$$
$$\mathbf{x}_{u\phi} = \begin{bmatrix} \mathbf{u} \\ \boldsymbol{\phi} \end{bmatrix} \qquad \mathbf{f}_{u\phi} = \begin{bmatrix} \mathbf{f}_s \\ \mathbf{f}_\phi \end{bmatrix}, \tag{41}$$

where $\dot{\mathbf{f}}_\phi = \mathbf{f}_a$. Note that also for $\mathbb{E}_{u\phi}$ and $\mathbb{A}_{u\phi}$, the matrices of the equivalent descriptor system are indefinite such that stability is not preserved in a one-sided projection.

It is shown in [52] that by changing the sign of the set of equations governing the acoustic degrees of freedom, resulting in the so-called modified $u-\phi$, leads to global symmetric positive definite $\mathbf{M}_{mu\phi}$ and $\mathbf{K}_{mu\phi}$ and positive semi-definite $\mathbf{C}_{mu\phi}$, ensuring that the conditions for stability for the equivalent descriptor formulation are fulfilled. Even though the modified $u-\phi$ formulation lacks symmetry as compared to the standard $u-\phi$ formulation, a one-side projection-based MOR preserves stability and the resulting reduced-order models are well suited for time domain simulation.

5.1.3 Extended projection basis preserving stability using the $u-p$ formulation

As the poles of the $u-p$ formulation and the modified $u-\phi$ formulation are equal as shown in [52], stability should also be preserved when converting a system from the $u-p$ formulation to the $u-\phi$ formulation and vice versa. In order to do so, the block-partitioned structure is required, which gets lost in the reduction process. By carefully selecting the structure of the projection basis,

the block structure within the second order system matrices can be retained, allowing for this conversion between both formulations.

Let the regular projection basis $\mathbf{V} \in \mathbb{C}^{n \times k}$, obtained through any one-sided projection-based MOR method (e.g. Krylov subspace projection, modal truncation, ...), be given by

$$\mathbf{V} = \begin{bmatrix} \mathbf{V}_s \\ \mathbf{V}_a \end{bmatrix}, \tag{42}$$

with $\mathbf{V}_s \in \mathbb{C}^{n_s \times k}$ the part of the projection matrix that corresponds to the structural degrees of freedom and $\mathbf{V}_a \in \mathbf{C}^{n_a \times k}$ the part corresponding to the acoustic degrees of freedom. By augmenting this projection basis with zero blocks, and extend projection $\widetilde{\mathbf{V}}$

$$\widetilde{\mathbf{V}} = \begin{bmatrix} \mathbf{V}_s & 0 \\ 0 & \mathbf{V}_a \end{bmatrix} \tag{43}$$

is obtained that achieves block structure preserving MOR for coupled systems, similar as the approach presented in [5]. The space spanned by the columns of $\widetilde{\mathbf{V}}$ contains the space spanned by the columns of $\mathbf{V}$, such that when using $\widetilde{\mathbf{V}}$ the reduced system will be at least as accurate as when using $\mathbf{V}$. For practical implementation it is recommended to orthogonalize $\widetilde{\mathbf{V}}$, which equates to orthogonalizing both $\mathbf{V}_s$ and $\mathbf{V}_a$. Also note that $\widetilde{\mathbf{V}}$ has twice as many columns as $\mathbf{V}$ such that the projected system will contain twice as many DOFs. Since $\mathbf{V}_s$ and $\mathbf{V}_a$ may be rank-deficient this can be slightly ameliorated by using a rank-revealing algorithm for the orthogonalization of $\mathbf{V}_s$ and $\mathbf{V}_a$, but in our experience the total number of columns in $\widetilde{\mathbf{V}}$ still remains close to twice the number of columns in $\mathbf{V}$.

5.1.4 Workflow

Both approaches, starting from the modified $u - \phi$ formulation and the $u - p$ formulation are summarised in Figure 7.

It is advisable to use the modified $u - \phi$ formulation for stability preserving MOR of coupled vibro-acoustic finite element models. Keeping the system in $u-p$ formulation necessitates the use of an extended projection basis $\widetilde{\mathbf{V}}$, resulting in a reduced-order model with possibly up to twice as many DOFs. This reduced order modeling approach was recently extended towards time-stable coupled exterior vibro-acoustic finite element simulations [53].

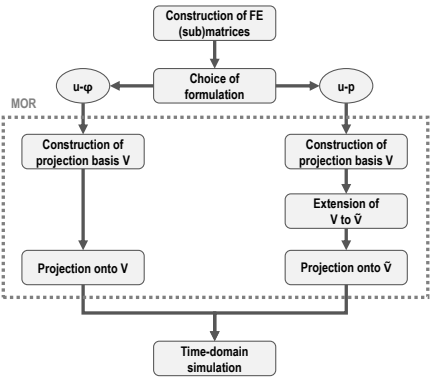


Fig. 7: Workflow for stability preserving vibro-acoustic model order reduction [52]

5.1.5 Calculation example - car interior with vibrating roof

As an example, the vibro-acoustic behaviour of a car interior is studied. The roof of the car is modeled as a flexible steel panel ($E = 200$ GPa, $\nu = 0.3$, $\rho = 8000$ kg/m^3, Rayleigh damping ($C_s = \alpha M_s + \beta K_s$) with $\alpha = 10$ and $\beta = 1 \cdot 10^{-7}$) with a thickness of 2 mm which is clamped at its boundaries and the interior is filled with air ($\rho = 1.225$ kg/m^3, $c = 340$ m/s). Linear elements are used with a resolution of at least six elements per wavelength up to 200 Hz. The resulting finite element mesh is shown in figure 8. Near the plate the mesh is more refined since the wavelength of the bending waves in the structure is smaller than the acoustic wavelength at 200 Hz. A normal impedance boundary condition of twice the characteristic impedance of air ($\mathrm{Z}_n = 2 \cdot 1.225 \cdot 340$ Pa·s/m) is imposed on the surfaces of the seats in the interior cavity. All other boundaries of the acoustic domain are considered rigid ($v_n = 0$ m/s). A point force at (1.50, 0.08, 1.09) m excites the structure and the sound pressure is calculated at (0.73, 0.23, 0.68) m.

The FE model of the roof and acoustic cavity consist of 7455 and 6583 DOFs, respectively. A one-sided Krylov subspace projection was constructed using SOAR [2, 56]. All reduced-order models consist of 60 DOFs, except for the $u - p$ projection with extended basis (equation 43)), which results in 120 DOFs.

Figures 9 and 10 show the frequency response functions and the relative error with the full model, obtained applying model order reduction on each of the models. All ROMs are able to accurately describe the full system behaviour in the frequency domain up to about 200 Hz. The $u - p$ projected system with the

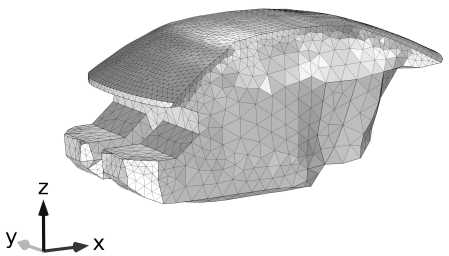


Fig. 8: Finite element mesh of the car interior geometry [52].

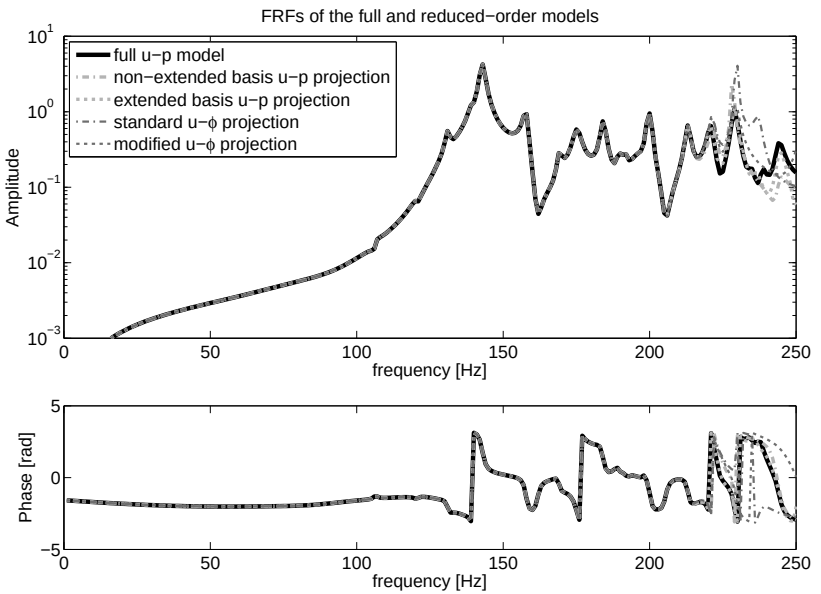


Fig. 9: Frequency response function of the car cavity model calculated with the full-order model and the reduced order models.

extended basis is more accurate than the reduced-order model that is obtained with the non-extended basis. Figure 11 shows the location of the poles of the reduced order models in the complex plane. Both the $u-p$ projection without

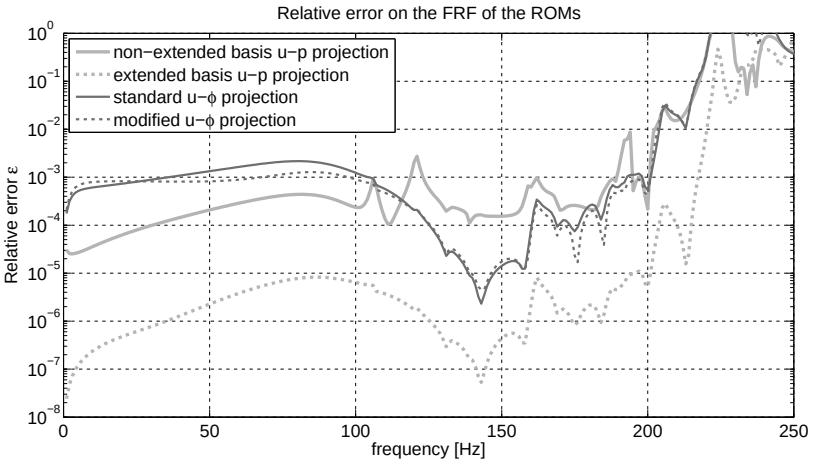


Fig. 10: Relative error on the amplitude of the frequency response function of the reduced-order models of the car cavity.

extended basis and the projection of the system in standard $u - \phi$ formulation lead to unstable reduced-order models.

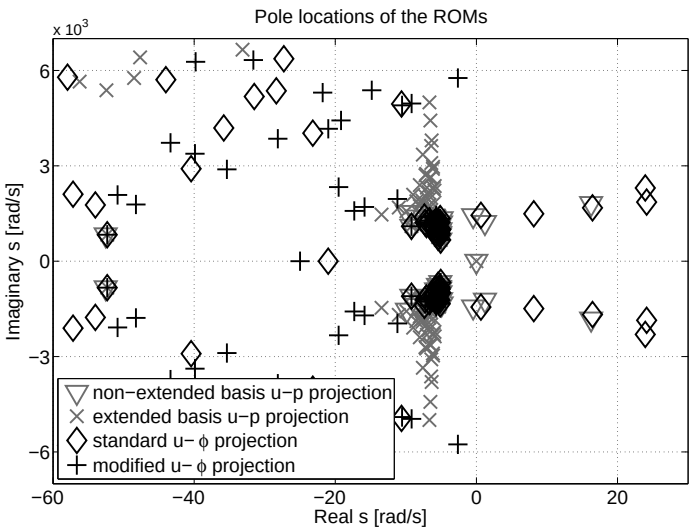


Fig. 11: Poles of the different ROMs of the car cavity models. The non-extended basis $u - p$ projection and standard $u - \phi$ projection result in unstable time-domain behaviour.

Finally, Figure 12 shows the convergence of the $\mathcal{H}_2$-norm of the relative frequency response function amplitude error ε of the different reduction methods, evaluated over the range of 1 to 200 Hz. The method using an extended projection basis performs substantially worse than the other methods when comparing them in terms of accuracy per DOFs.

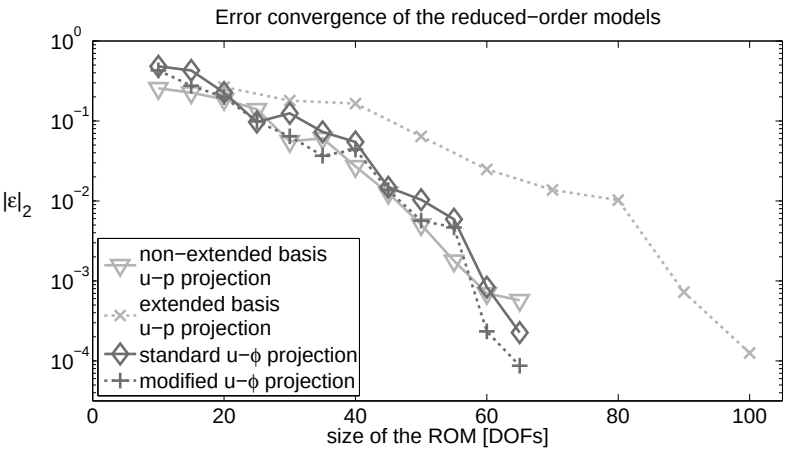


Fig. 12: Efficiency of the MOR methods in terms of accuracy per DOF for the car cavity vibro-acoustic model.

6 Conclusions

We presented an overview of methods for model order reduction of dynamical systems arising in (coupled) acoustics and vibrations problems encountered in mechanical engineering. The choice of methods took into account the a range of relevant requirements in practical engineering problems: computational efficiency, frequency limitation, stability, nonlinearity in the frequency variable, and preservation of underlying model structure.

For computational efficiency, the number of large sparse LU factorizations should be small. This can be achieved by using Krylov methods with a greedy selection of the interpolation points and using higher order Hermite interpolation. We advocate two-level reduced order modeling methods, where a (rational) Krylov method with greedy selection of (a small number of) shifts leads to a reduced

order model of moderate size. This reduced order model can be further reduced by applying balanced truncation, or methods in the Loewner framework.

In mechanical engineering models, the relevant structure can often be preserved by not building a frequency-linear reduced order model, but a model that respects the frequency dependency by projecting the system matrices on a well chosen block of the Krylov vectors.

Bibliography

[1] J.-F. Allard and N. Atalla. *Propagation of sound in porous media: modelling sound absorbing materials*. John Wiley & Sons, 2009.

[2] Z. Bai and Y. Su. Dimension reduction of second-order dynamical systems via a second-order Arnoldi method. *SIAM Journal on Matrix Analysis and Applications*, 26(5):1692–1709, 2005.

[3] A. Bayliss, M. Gunzburger, and E. Turkel. Boundary Conditions for the Numerical Solution of Elliptic Equations in Exterior Regions. *SIAM Journal on Applied Mathematics*, 42:430–451, 1982.

[4] A. Ben-Menahem and S.J. Singh. *Seismic Waves and Sources*. Springer Science & Business Media, 2012.

[5] P. Benner and L. Feng. Model order reduction for coupled problems. *Applied and Computational Mathematics: an international journal*, 14:3–22, 2015.

[6] P. Benner, P. Kürschner, and J. Saak. Frequency-limited balanced truncation with low-rank approximations. *SIAM Journal on Scientific Computing*, 38(1):A471–A499, 2016.

[7] P. Benner, V. Mehrmann, and D.C. Sorensen. *Dimension Reduction of Large-Scale Systems*. Springer, 2003.

[8] Jean-Pierre Berenger. A perfectly matched layer for the absorption of electromagnetic waves. *Journal of computational physics*, 114(2):185–200, 1994.

[9] B. Besselink, U. Tabak, A. Lutowska, N. van de Wouw, H. Nijmeijer, D.J. Rixen, M.E. Hochstenbach, and W.H.A. Schilders. A comparison of model reduction techniques from structural dynamics, numerical mathematics and systems and control. *Journal of Sound and Vibration*, 332(19):4403–4422, 2013.

[10] D.T. Blackstock. *Fundamentals of physical acoustics*. John Wiley & Sons, New York, 2000.

[11] D. Colton and R. Kress. *Inverse acoustic and electromagnetic scattering theory*. Springer-Verlag, Berlin, Heidelbert, New York, 2nd edition, 1998.

[12] A. Craggs. The transient response of a coupled plate-acoustic system using plate and acoustic finite elements. *Journal of Sound and Vibration*, 15(4):509–528, 1971.

[13] R. R. Craig and M. Bampton. Coupling of substructures in dynamic analysis. *AIAA Journal*, 6(7):1313–1321, 1968.

[14] E. Deckers, S. Jonckheere, D. Vandepitte, and W. Desmet. Modelling techniques for vibro-acoustic dynamics of poroelastic materials. *Archives of Computational Methods in Engineering*, 22(183-236), 2015.

[15] G. Duan. *Analysis and Design of Descriptor Linear Systems*. Springer, 2010.

[16] G.C. Everstine. A symmetric potential formulation for fluid-structure interaction. Letter to the editor. *Journal of Sound and Vibration*, 79:157–160, 1981.

[17] J.D. Ferry. *Viscoelastic Properties of Polymers*. John Wiley & Sons, New York, 1980.

[18] R. Freymann. *Advanced numerical and experimental methods in the field of vehicle structural-acoustics*. Hieronymus Buchreproduktions GmbH, 2000.

[19] S. W. Gaaf and E. Jarlebring. The infinite bi-Lanczos method for nonlinear eigenvalue problems. *SIAM Journal on Scientific Computing*, 39(5):S898–S919, 2017.

[20] U. Hetmaniuk, R. Tezaur, and C. Farhat. Review and assessment of interpolatory model order reduction methods for frequency response structural dynamics and acoustics problems. *International Journal for Numerical Methods in Engineering*, 90:1636–1662, 2012.

[21] W. C. Hurty. Dynamic analysis of structural systems using component modes. *AIAA Journal*, 3(4):678–685, 1965.

[22] E. Jarlebring, K. Meerbergen, and W. Michiels. An Arnoldi like method for the delay eigenvalue problem. *SIAM Journal on Scientific Computing*, 32(6):3278–3300, 2010.

[23] S. Jonckheere, E. Deckers, and W. Desmet. A matrix-free model order reduction scheme for vibro-acoustic systems including complex noise control treatments. In *Proceedings of Internoise2018, 26-29 August 2018, Chicago, US*, 2018.

[24] M. Lehner and P. Eberhard. A two-step approach for model reduction in flexible multibody dynamics. *Multibody Syst Dyn*, 17(2-3):157–176, 2007.

[25] X. Li. *Power flow prediction in vibrating systems via model reduction*. PhD thesis, Boston University, College of Engineering, 2004.

[26] P. Lietaert and K. Meerbergen. Comparing Loewner and Krylov based model order reduction for time delay systems. In *Proceedings of the European Control Conference 2018*, 2018.

[27] P. Lietaert, K. Meerbergen, J. Perez, and B. Vandereycken. Automatic rational approximation and linearization of nonlinear eigenvalue problems. Technical Report arXiv:1801.08622, 2018. Submitted for publication.

[28] P. Lietaert, K. Meerbergen, and F. Tisseur. Compact two-sided Krylov metods for nonlinear eigenvalue problems. *SIAM Journal on Scientific Computing*, 40(5):A2801–A2829, 2018.

[29] D. Lu, Y. Su, and Z. Bai. Stability analysis of two-level orthogonal Arnoldi

procedure. *SIAM Journal on Matrix Analysis and Applications*, 37(1):192–214, 2016.

[30] R. Lyon and R. DeJong. *Theory and application of statistical energy analysis*. Butterworth-Heinemann, 2nd edition, 1995.

[31] Mardochée Magolu monga Made, Robert Beauwens, and Guy Warzée. Preconditioning of discrete Helmholts operators perturbed by a diagonal complex matrix. *Communications in Numerical Methods in Engineering*, 16:801–817, 2000.

[32] S. Marburg. Six boundary elements per wavelength: is that enough? *Journal of Computational Acoustics*, 10:25–51, 2002.

[33] A.J. Mayo and A.C. Antoulas. A framework for the solution of the generalized realization problem. *Linear Algebra and its Applications*, 425(2):634 – 662, 2007.

[34] K. Meerbergen and Z. Bai. The Lanczos method for parameterized symmetric linear systems with multiple right-hand sides. *SIAM Journal on Matrix Analysis and Applications*, 31(4):1642–1662, 2010.

[35] K. Meerbergen and J.P. Coyette. Connection and comparison between frequency shift time integration and a spectral transformation preconditioner. *Numerical Linear Algebra with Applications*, 16:1–17, 2009.

[36] W. Michiels, G. Hilhorst, G. Pipeleers, T. Vyhlídal, and J. Swevers. Reduced modelling and fixed-order control of delay systems applied to a heat exchanger. *IET Control Theory & Applications*, 2017.

[37] W. Michiels, E. Jarlebring, and K. Meerbergen. Krylov based model order reduction of time-delay systems. *SIAM Journal on Matrix Analysis and Applications*, 32(4):1399–1421, 2011.

[38] COMSOL Multiphysics, 2018. https://www.comsol.com/model/sedan-interior-acoustics-15013.

[39] MUMPS. MUlfrontal Massively Parallel Solver, 2009. http://graal.ens-lyon.fr/MUMPS/.

[40] Y. Nakatsukasa, O. Sète, and L. N. Trefethen. The AAA algorithm for rational approximation. *SIAM Journal on Scientific Computing*, 40(3):A1494–A1522, 2018.

[41] J. Peeters and W. Michiels. Computing the H2 norm of large-scale time-delay systems. In *Proceedings of the IFAC Joint conference, Grenoble, 2013*, volume 11, pages 114–119, 2013.

[42] A. Pierce. *Acoustics: An Introduction to Its Physical Principles and Applications*. McGraw-Hill series in mechanical engineering, McGraw-Hill, 1981.

[43] R.S. Puri, D. Morrey, A.J. Bell, J.F. Durodola, E.B. Rudnyi, and J.G. Korvink. Reduced order fully coupled structural–acoustic analysis via

implicit moment matching. *Applied Mathematical Modelling*, 33:4097–4119, 2009.

[44] M.D. Rao. Recent applications of viscoelastic damping for noise control in automobiles and commerical airplanes. *Journal of Sound and Vibratiion*, 262:457–474, 2003.

[45] W. Desmet S. Jonckheere, X. Li. A matrix-free model order reduction scheme for vibro-acoustic problems with complex damping treatments. In *Proceedings of ISMA2016, Leuven, 19-21 September 2016, Leuven, Belgium*, 2016.

[46] M. Saadvandi, K. Meerbergen, and W. Desmet. Parametric dominant pole algorithm for parametric model order reduction. *Journal of Computational and Applied Mathematics*, 295:259–280, 2014.

[47] R.D. Slone, R. Lee, and J.-F. Lee. Multipoint Galerkin asymptotic waveform evaluation for model order reduction of frequency domain FEM electromagnetic radiation problems. *IEEE Transactions on Antennas and Propagation*, 49(10):1504–1413, 2001.

[48] W. Soedel. *Vibrations of Shells and Plates*. CRC Press, 2004.

[49] Y. Su and Z. Bai. Solving rational eigenvalue problem via linearization. *SIAM Journal on Matrix Analysis and Applications*, 32(1):201–216, 2011.

[50] R. Van Beeumen, K. Meerbergen, and W. Michiels. Compact rational Krylov methods for nonlinear eigenvalue problems. *SIAM Journal on Matrix Analysis and Applications*, 36(2):820–838, 2015.

[51] R. Van Beeumen, K. Van Nimmen, G. Lombaert, and K. Meerbergen. Model reduction for dynamical systems with quadratic output. *International Journal of Numerical Methods in Engineering*, 91(3):229–248, 2012.

[52] A. van de Walle, F. Naets, E. Deckers, and W. Desmet. Stability-preserving model order reduction for time-domain simulation of vibro-acoustic FE models. *International Journal for Numerical Methods in Engineering*, 109(6):889–912, 2017.

[53] S. van Ophem, O. Atak, E. Deckers, and W. Desmet. Stable model order reduction for time-domain exterior vibro-acoustic finite element simulations. *Computer Methods in Applied Mechanics and Engineering*, 325:240–264, 2017.

[54] K. Vergote. *Dynamic analysis of structural components in the mid frequency range using the wave based method, Non-determinism and inhomogeneities*. KULeuven, division PMA, PhD. thesis 2012D03, 2012.

[55] O. Von Estorff. *Boundary Elements in Acoustics: Advances and Applications*. WITpress, 2000.

[56] S. Wyatt. *Issues in Interpolatory Model Reduction: Inexact Solves, Second-*

order Systems and DAEs. PhD thesis, Faculty of the Virginia Polytechnic Institute and State University, 2012.

[57] X. Xie, Z. Hui, S. Jonckheere, A. van de Walle, B. Pluymers, and W. Desmet. Adaptive model reduction technique for large-scale dynamical systems with frequency-dependent damping. *Computer Methods in Applied Mechanics and Engineering*, 332:363–381, 2018.

[58] Y. Yue and K. Meerbergen. Accelerating optimization of parametric linear systems by model order reduction. *SIAM Journal on Optimization*, 23(2):687–1370, 2013.

[59] Matthew J. Zahr, Philip Avery, and Charbel Farhat. A multilevel projection-based model order reduction framework for nonlinear dynamic multiscale problems in structural and solid mechanics. *International Journal for Numerical Methods in Engineering*, 2017.

[60] O. C. Zienkiewicz, R.L. Taylor, J.Z. Zhu, and P. Nithiarasu. *The Finite Element Method - The three volume set*. Butterworth-Heinemann, 6th edition, 2005.